CENTRAL RESEARCH LIBRARY
DOCUMENT COLLECTION

107

MARTIN MARIETTA ENERGY SYSTEMS LIBRARIES
3 4456 0361447 1

ORNL-2865
UC-81 - Reactors-Power

MARITIME REACTOR PROJECT

ANNUAL PROGRESS REPORT

FOR PERIOD ENDING NOVEMBER 30, 1959

CENTRAL RESEARCH LIBRARY
DOCUMENT COLLECTION
LIBRARY LOAN COPY
DO NOT TRANSFER TO ANOTHER PERSON
If you wish someone else to see this document, send in name with document and the library will arrange a loan.

OAK RIDGE NATIONAL LABORATORY
operated by
UNION CARBIDE CORPORATION
for the
U.S. ATOMIC ENERGY COMMISSION

Printed in USA. Price $2.25. Available from the

Office of Technical Services
Department of Commerce
Washington 25, D.C.

LEGAL NOTICE

This report was prepared as an account of Government sponsored work. Neither the United States, nor the Commission, nor any person acting on behalf of the Commission:

A. Makes any warranty or representation, expressed or implied, with respect to the accuracy, completeness, or usefulness of the information contained in this report, or that the use of any information, apparatus, method, or process disclosed in this report may not infringe privately owned rights; or

B. Assumes any liabilities with respect to the use of, or for damages resulting from the use of any information, apparatus, method, or process disclosed in this report.

As used in the above, "person acting on behalf of the Commission" includes any employee or contractor of the Commission, or employee of such contractor, to the extent that such employee or contractor of the Commission, or employee of such contractor prepares, disseminates, or provides access to, any information pursuant to his employment or contract with the Commission, or his employment with such contractor.

cy. 107

Report No.: ORNL-2865 Classification: Unclassified

Author(s):

Subject: Maritime Reactor Project Annual Progress Report for Period Ending November 30, 1959.

Request compliance with indicated action:

Please remove the following pages from your copy of the subject report. Pages 7 and 8, 37 and 38 and replace them with the attached corrected pages.

replaced by errata dated Feb. 19, 1960

N. T. Bray, Supervisor
Laboratory Records Department
Technical Information Division

NTB:WCB:jlb

ORNL:RC

X-847

INTRA-LABORATORY CORRESPONDENCE

OAK RIDGE NATIONAL LABORATORY

February 19, 1960

CPL

Report No.: ORNL-2865 Copy: 107 Classification: Unclassified

Author(s):

Subject: Maritime Reactor Project Annual Progress Report for Period Ending November 30, 1959.

Request compliance with indicated action:

Please remove page 37-38 from your copy of the subject report, and replace it with the attached revised page.

N. T. Bray, Supervisor
Laboratory Records Department
Technical Information Division

NTB:WCB:jlb

ORNL:RC

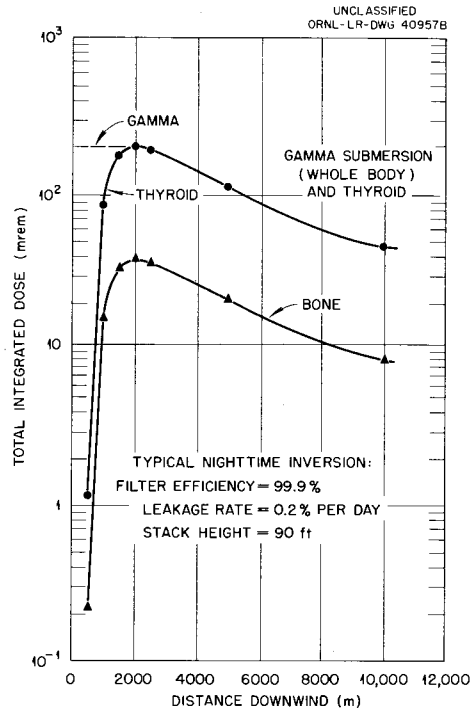

Fig. 1.1. Total Integrated Dose in 24 hr from Continuous Elevated Source During Nighttime Inversion.

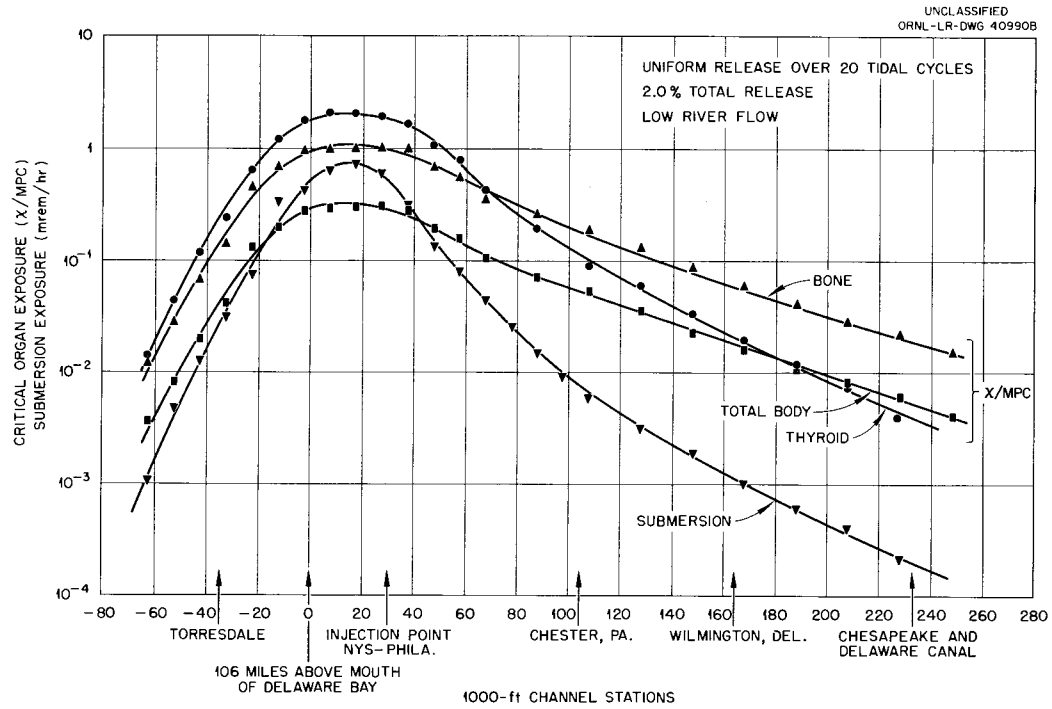

Fig. 1.2. Maximum Exposure as a Function of River Location.

rather to assure that the exposure would be as low as practical. The result has been the reduction of credible accident exposures to exceptionally low values.

While most of the foregoing conclusions were based upon consideration of the maximum credible accident, the various accidents considered in the enviromental study included many less serious accidents, all of which could result in the release of some activity to the environment. No attempt was made to consider all possible accidents individually; however, accidents representative of a number of different situations were studied. In all instances the amount of activity released vs time for a particular accident was taken to be that given in Babcock & Wilcox Company reports. Although in the initial stages of testing and operation, the activity buildup in each of the various systems and components will be far from the maximum design value, all analyses were carried out using the maximum activity levels except where otherwise stated. The accidents considered included the following: (1) inadvertent release of gaseous activity, (2) rupture of the double-bottom tanks, (3) spill of the ion-exchange resin, (4) damage to a fuel element during refueling, (5) the maximum credible accident with the ship afloat, (6) the maximum credible accident with the ship sunk, and (7) variations of the maximum credible accident in which the containment vessel was voided.

The Babcock & Wilcox Company analysis demonstrated that no accident occurring within the container could cause its rupture, while a George G. Sharp study showed that no ship accident in confined water could either rupture the containment vessel or initiate the maximum credible accident. Examination of the presumed course of the maximum credible accident reveals that a more serious accident is conceivable; that is, the containment vessel closure might be voided at the same time as the maximum credible accident, either as a consequence of the same accident or otherwise. There are two instances in which the container might be open during the course of the maximum credible accident; namely, (1) a ship collision on the high seas and (2) the containment vessel being opened to soon after shutdown.

ORNL-2865

Reactors—Power
TID-4500 (15th ed.)

CONTRACT NO. W-7405-ENG-26

MARITIME REACTOR PROJECT

ANNUAL PROGRESS REPORT

for Period Ending November 30, 1959

A. L. Boch, Project Coordinator

DATE ISSUED

JAN 14 1960

OAK RIDGE NATIONAL LABORATORY
Oak Ridge, Tennessee
operated by
UNION CARBIDE CORPORATION
for the
U. S. ATOMIC ENERGY COMMISSION

3 4456 0361447 1

CONTENTS

INTRODUCTION AND SUMMARY 1

1. SAFETY ANALYSES 4

Environmental Analysis of N.S. Savannah Operation at Camden 4

Health Physics Manual 9

Evaluation of the Safety System of the N.S. Savannah by Means of the ORNL Analog Computer 10

Examination of the N.S. Savannah Reactor Training Simulator .. 10

2. WASTE DISPOSAL 11

Resin Disposal in Concrete 11

Demineralizer Resin Studies 12

3. PRESSURIZED-WATER IN-PILE TEST LOOP 17

Flux Measurements 36

4. METALLURGY 41

Rotary Swaging of Stainless Steel-Clad UO_2 Fuel Rods 41

Effect of Type of Oxide Density 41
Effect of Swaging Temperature on Oxide Properties 41
Evaluation of Commercially Produced Swageable Grades of UO_2 44
Fabrication of Swaged Rods Into Fuel Bundle 45
Swaging of Small-Diameter Rods 45
Swaging Fuel Tubes Clad Internally and Externally 48

Compartmented Fuel Plate Development 50

Metal Heat Transfer Bonds 55

Irradiation Studies 62

Analysis of Primary System Components for Cobalt and Other Trace Elements 64

Evaluation of Brittle Fracture Characteristics of the N.S. Savannah Pressure Vessel 64

Electroless-Nickel Brazing Studies 66

Pyrometer Wire Studies 68

5. PHYSICS 69

MARITIME REACTOR PROJECT ANNUAL PROGRESS REPORT

INTRODUCTION AND SUMMARY

The ORNL Maritime Reactor Project was initiated in September 1957 for the purpose of providing technical support to the Office of Maritime Reactors of the Division of Reactor Development (AEC) in the development of nuclear-powered merchant ships. This support has consisted of: (1) review and technical advisory service and (2) supplementary studies, experimental programs, and specialized services. The Laboratory's efforts have been mainly directed toward assistance to the N.S. Savannah project, although some have more general application. It should also be noted that, although the Laboratory's activities cover a wide spectrum of reactor technology, the total effort does not constitute a complete and integrated program of reactor development. In general, developmental activities and studies are limited both in scale and scope to meet immediate needs in selected areas.

The status of the N.S. Savannah project is summarized briefly in the following statements. Design and fabrication of the reactor and propulsion equipment by Babcock & Wilcox Company of Lynchburg, Virginia, are nearing completion. The ship, which is being built by the New York Shipbuilding Corporation of Camden, New Jersey, was launched on July 21, 1959; and installation of the nuclear power plant is well advanced. Initial tests and trials are expected to extend from six months to one year beginning in the early part of 1960. States Marine Corporation of Deleware, who will operate the ship as an agent of the Maritime Administration, has been participating in the program since July 1958.

During the annual period ending November 30, 1959, the nature of the ORNL supporting activities gradually changed, reflecting the progress in the construction of the N.S. Savannah. Design reviews continued to require considerable attention. Approximately 230 specifications, drawings, reports, and other documents were reviewed, and comments were submitted to the AEC. Near the end of the current report period, review

of the Savannah reactor design on an over-all routine basis was greatly curtailed as the design became fixed. This effort was partially replaced by review assistance on the second core and on the startup test program. In September 1959, one ORNL engineer was assigned to the AEC-MARAD group at the Shipyard to assist in the planning and execution of the startup test program.

The Inspection Engineering Department of the Laboratory continued to act as an inspection agency for the AEC, witnessing inspections and tests during fabrication of components of the nuclear reactor system. This work has included full-time resident inspection for considerable periods at: (1) the Babcock & Wilcox plant in Barberton, Ohio, where primary system components were fabricated; (2) the Babcock & Wilcox plant in Lynchburg, Virginia, where fuel elements and other core components are being fabricated; (3) the General Electric plant in San Jose, California, where the control rod drive mechanisms are being built; and (4) the Allis-Chalmers plant in Milwaukee, Wisconsin, where the primary coolant pumps are being built. In addition, inspection was performed on a large number of other components in vendor's plants; and one ORNL inspector is assigned to the Maritime Administration at the Shipyard to assist during reactor installation.

ORNL is participating in an on-the-job training program for personnel enrolled in the U. S. Maritime Reactor Training School at Lynchburg, Virginia. Ten participants from the school began a three-month on-the-job training session in October 1959.

An environmental analysis was made of safeguard aspects of operation of the N.S. Savannah at the New York Shipbuilding Corporation site in Camden, New Jersey. The consequences of the release of activity to the environment in the case of the maximum credible accident were examined, and the calculated exposures were found to be extremely low. A study of the safety response of the N.S. Savannah reactor on the ORNL Analog Computer further defined the important role of the Doppler coefficient in controlling reactivity excursions. Health physics aspects of the operation of a nuclear-powered vessel of the N.S. Savannah type were

studied, and an extensive compilation of pertinent information and recommendations for a shipboard health physics program was prepared. Limited waste disposal studies indicated that sea disposal of exhausted demineralizer resins may be facilitated by casting the radioactive resins into concrete.

Installation of a pressurized-water in-pile test loop in the Oak Ridge Research Reactor neared completion. The neutron flux distribution in the loop was determined by experimental measurements in a nuclear mockup of the in-pile section.

Metallurgical activities in direct support of the N.S. Savannah included nil-ductility testing of steel from the reactor vessel, chemical analyses of primary system components, and investigations of the properties of electroless-nickel brazed joints. Limited fabrication studies were carried out on advanced fuel concepts which may have merit for future cores of the Savannah reactor. Most of the latter effort was applied to swaged UO_2 rod-type elements.

A series of physics calculations is being carried out in an attempt to evaluate the possible advantages of using Zircaloy instead of stainless steel as the structural material for Core III of the Savannah. To be meaningful, such calculations must be done in considerable detail to account for the numerous heterogeneities in the core. Proposed calculational methods were checked against critical experiment data. Use of Zircaloy instead of stainless steel for the fuel element cans was found to result in a marked reduction in enrichment for a given initial cold reactivity. The effect of this substitution on control rod worth, temperature coefficients, and lifetime has not yet been determined.

1. SAFETY ANALYSES

Environmental Analysis of N.S. Savannah Operation at Camden

At the request of the Office of Maritime Reactors, an analysis[1] was made of the possible consequences of the accidental release of activity from the N.S. Savannah. The results of this study, which are a vital part of the complete hazards analysis, describe the possible consequence of credible releases of activity to the environment of the proposed start-up site, the New York Shipbuilding Company yards at Camden, New Jersey. The credible sources of activity release and, in particular, the maximum credible accident have been defined by the Babcock & Wilcox Company.[2]

The N.S. Savannah is subject to most of the "conventional" reactor accidents and failures and, in addition, is subject to all the hazards of a ship at sea. The designers of the vessel have been quite successful in an attempt to preclude the possibility that the reactor and ship hazards would be additive. The N.S. Savannah has been designed so that no ship accident in confined waters can induce the maximum credible reactor accident; however, it is conceivable that such an accident could occur on the high seas.

This analysis of the consequence of release of activity to the environment surrounding the Camden site is unique in that the possibility of release to the hydrosphere has been as important a consideration as release to the atmosphere. The significant information which permitted confident evaluation of the activity concentrations in the Delaware River following assumed releases was provided by data obtained on the dispersion of dye in a model of the river. The model was constructed and the dye tests were run by the U. S. Army Corps of Engineers.

---

[1]W. B. Cottrell, L. A. Mann, F. L. Parker, and G. D. Schmidt, Environmental Analyses of N.S. Savannah Operation at Camden, ORNL CF-59-9-9 (rev), November 6, 1959.

[2]Nuclear Merchant Ship Reactor Project Preliminary Safeguards Report, BAW-1117, Vol. 1 (rev), September 15, 1958, and Vol. II, November 3, 1958.

The ability to contain activity which might be released from the fuel in the event of a reactor accident is one of the most important features of any reactor system. The proposed design of the nuclear plant aboard the N.S. Savannah will provide a very high degree of containment. In addition to the containment barriers provided by the fuel cladding and the primary system, the plant is enclosed in a steel pressure-containment vessel, and this vessel in turn in located in an isolated hold of the ship which is maintained at a negative pressure. The air in this hold is continuously filtered and discharged to the ship's stack. Thus the two most effective "containment techniques" yet devised are employed in series.

In undertaking this environmental analysis, the various possible accidents were examined first to be certain that the important or controlling hazards were considered. The resulting activity concentrations and the potential exposure as a consequence of the release of the activity to either the air or river water were estimated. The exposure information was then evaluated and related to the area and persons affected in order to arrive at a comprehensive evaluation of the hazards associated with the release of activity.

The maximum credible accident has been set forth as the series of events which could follow a rupture in the primary water coolant system. Loss of the coolant would result in increased temperature of the fuel and eventual rupture of the fuel element cladding. Still later, gradual melting of the UO_2 fuel would occur and fission products would be released from the fuel in proportion to their volatility, as modified by their chemical characteristics. Homogeneous mixing of the escaped fission products with the gases and vapors inside the containment vessel was assumed in the analysis.

Calculated atmospheric releases following the maximum credible accident were evaluated for typical lapse and inversion conditions. The consequences of deposition and rainout, as well as release at ground level and stack height, both with and without the stack filter, were considered, and total integrated doses for 24-hr continuous exposures were

computed. The total integrated dose for the nighttime inversion condition as a function of distance from the stack is shown in Fig. 1.1. The maximum dose following 24-hr exposure would be only 200 mr.

In view of the long half-life for the residence of any contamination in a tidal estuary, it is fortunate that the activity concentrations that would be found in the water following the accidental release of activity would be low. This is illustrated in Fig. 1.2 in which the maximum exposure as a function of river location is shown for the uniform release of 2% of the total activity over 20 tidal cycles. Even for such an extreme case as this, the maximum permissible concentration values would be exceeded by only a factor of 2.

As a consequence of the design and environmental safety features, it is not surprising that the off-site exposures following even the maximum credible reactor accident would be very low. The calculated total integrated dose from atmospheric contamination following this accident at the point of maximum ground concentration during the inversion condition would be 200 mr, the maximum total exposure to the populace from such an incident would be 4000 man-rem, and the consequent genetic dose to the populace of the United States would be 2×10^{-5} rem. Were this same accident to release the activity to the river rather than to the atmosphere, the resulting maximum concentration (temporary) would be less than a factor of 2 above the maximum permissible concentration for continuous occupational exposure. This concentration level might persist for several days, but the peak would not occur near the intake of any municipal water supply.

These analyses are not without some uncertainties, such as the rate and the total fraction of activity release from the fuel, the fraction deposited before reaching the filter, the fraction removed by the filter, and the assumed meteorological conditions. The calculated exposures are so low, however, that increases by an order of magnitude would not significantly alter the argument. The reason for this is simple; the N.S. Savannah containment was not designed to limit exposure as a result of the maximum credible accident to a particular permissible value, but

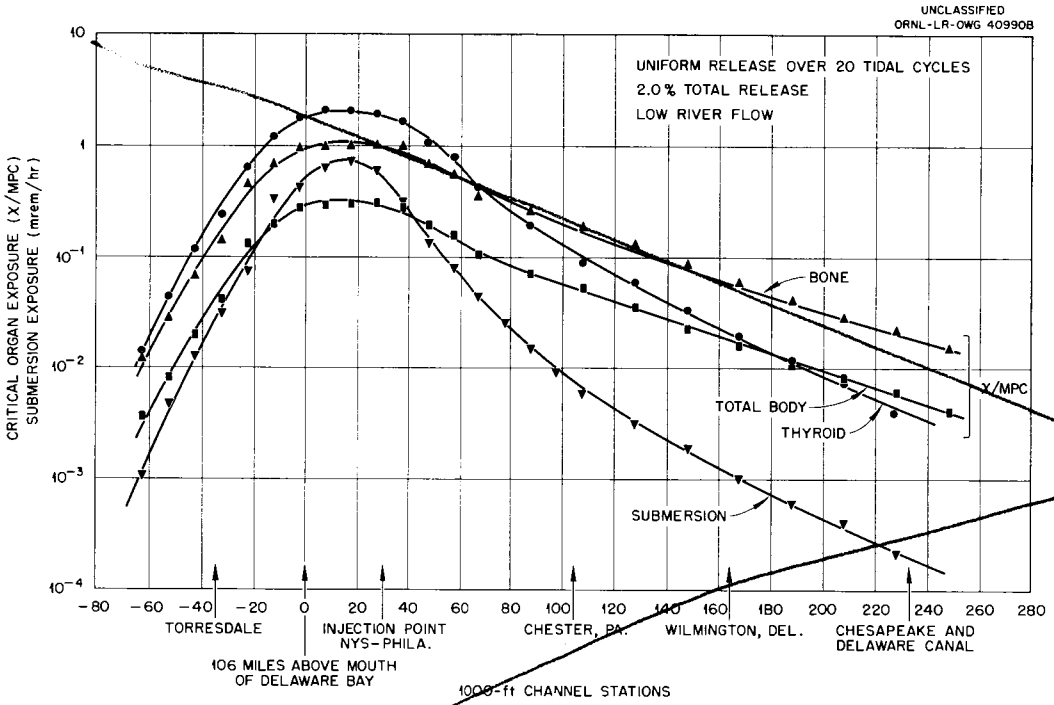

Fig. 1.1. Total Integrated Dose in 24 hr from Continuous Elevated Source During Nighttime Inversion.

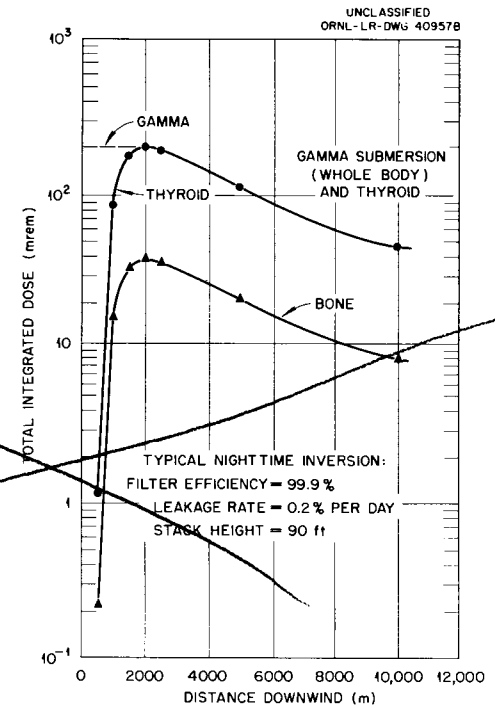

Fig. 1.2. Maximum Exposure as a Function of River Location.

rather to assure that the exposure would be as low as practical. The result has been the reduction of credible accident exposures to exceptionally low values.

While most of the foregoing conclusions were based upon consideration of the maximum credible accident, the various accidents considered in the enviromental study included many less serious accidents, all of which could result in the release of some activity to the environment. No attempt was made to consider all possible accidents individually; however, accidents representative of a number of different situations were studied. In all instances the amount of activity released vs time for a particular accident was taken to be that given in Babcock & Wilcox Company reports. Although in the initial stages of testing and operation, the activity buildup in each of the various systems and components will be far from the maximum design value, all analyses were carried out using the maximum activity levels except where otherwise stated. The accidents considered included the following: (1) inadvertent release of gaseous activity, (2) rupture of the double-bottom tanks, (3) spill of the ion-exchange resin, (4) damage to a fuel element during refueling, (5) the maximum credible accident with the ship afloat, (6) the maximum credible accident with the ship sunk, and (7) variations of the maximum credible accident in which the containment vessel was voided.

The Babcock & Wilcox Company analysis demonstrated that no accident occurring within the container could cause its rupture, while a George G. Sharp study showed that no ship accident in confined water could either rupture the containment vessel or initiate the maximum credible accident. Examination of the presumed course of the maximum credible accident reveals that a more serious accident is conceivable; that is, the containment vessel closure might be voided at the same time as the maximum credible accident, either as a consequence of the same accident or otherwise. There are two instances in which the container might be open during the course of the maximum credible accident; namely, (1) a ship collision on the high seas and (2) the containment vessel being opened to soon after shutdown.

See errata

Since less than 2% of the world's merchant fleet is capable of causing containment rupture by collision on the open sea and could cause it then only if the colliding ship were to strike the N.S. Savannah in the reactor compartment, the probability of such an accident is very small. The area seriously contaminated by such an accident would be large, but, in general, would be confined to the open sea.

On the other hand, if the containment vessel were opened for maintenance while the reactor was shut down in port, it is conceivable that the primary system might rupture and release activity directly from the open containment vessel to the atmosphere. The occurrence of such an accident must be precluded by an administrative procedure which must not permit the containment vessel to be opened until the reactor has been allowed to cool for a sufficient time so that in the subsequent event of a primary system rupture there would be time to reseal the containment vessel before fuel element melting began to occur. This waiting time is a function of both reactor power and operating time, but fortunately it is sufficiently short in any case not to impose a serious restriction on ship maintenance.

Health Physics Manual

A Health Physics Manual[3] for the N.S. Savannah was completed on May 28, 1959, and transmitted to the Savannah Project Branch (AEC). This manual followed closely the outline presented in the previous report.[4] It is no longer the intention of the Savannah Project Branch to issue the manual in its present form; rather they have proposed that the health physicist employed by the ship operator, States Marine Corporation, utilize the material therein to construct detailed operating procedures for shipboard use.

---

[3]T. J. Burnett, C. E. Haynes, and E. J. Kuna, Health Physics Recommendations for the Operation of the NS Savannah, May 28, 1959.

[4]Maritime Reactor Project Annual Progress Report for Period Ending November 30, 1958, ORNL-2657, p 9.

Evaluation of the Safety System of the N.S. Savannah by Means of the ORNL Analog Computer

Nuclear excursions of the type that might occur during a reactor startup accident or following the stepwise injection of excess reactivity in the N.S. Savannah reactor were investigated with the use of the ORNL analog facility. It was found that the rate at which the automatic control system adds excess reactivity to the reactor is not a factor in the evaluation of the safety system, so long as the total excess reactivity available to the automatic system at no time exceeds that required to take the steady-state power above 130% of maximum operating power. This conclusion is possible because of the Doppler fuel temperature coefficient of reactivity present in the N.S. Savannah reactor. For this analysis, a Doppler coefficient of -1×10^{-5} in excess reactivity for each Fahrenheit degree was used. For larger magnitudes of the Doppler coefficient, the conclusion is also valid. On the basis of this analysis, a means for limiting the excess reactivity available to the automatic controller was described that is extremely simple and precise.

Examination of the N.S. Savannah Reactor Training Simulator

The N.S. Savannah reactor training simulator was reviewed and found to have insufficient basic analog computing equipment. It was recommended that the number of chopper-stabilized amplifiers for simulating the reactor be increased to approximately 120.

2. WASTE DISPOSAL

There will be three specific sources of radioactive wastes aboard a nuclear-powered merchant ship of the N.S. Savannah type. These sources, as described previously,[1] are the ion-exchange resins in the primary purification loop demineralizers, the radioactive gases, and the liquid wastes accumulated from the primary coolant blowdown water, the laboratory, and the shield water. In the investigation of an optimum waste disposal procedure, the experimental program has centered on disposal of the ion-exchange resins, because the resins in the demineralizers will be the source of the highest concentration of radioactive waste and because the most promising method of disposal of the radioactive liquid wastes involves the concentration of the activity with the use of ion-exchange units. The resins of ion-exchange units used for concentrating the activity of the liquid wastes would, of course, present an additional disposal problem.

Resin Disposal in Concrete

There are several possible methods for disposal of the resin beds, and, although discharge directly into the ocean is possible,[2] it would be advisable to release the activity in controlled amounts. Such control is readily and simply obtainable by mixing thoroughly the resin and ordinary Portland cement, in a ratio of about 1:2, with just enough water to make a workable mud. Experimental results indicate that concrete blocks prepared in this manner will have high integrity to physical shock and low leachability when contacted with a simulated sea water (0.55 M Cl^-, 0.47 M Na^+, 0.05 M Mg^{++}, 0.03 M $S^=$, 0.01 M Ca^{++}, and 0.01 M K^+) over extended periods of time. An experimental block was prepared

[1] Maritime Reactor Project Annual Progress Report for Period Ending November 30, 1958, ORNL-2657, p 6.

[2] Radioactive Waste Disposal from Nuclear-Powered Ships, Publication 658, National Academy of Sciences — National Research Council, Washington, D. C., 1959.

by mixing 120 ml of mixed-bed ion-exchange resin containing approximately 10 mc of mixed fission products ($\sim 1.5 \times 10^9$ gamma counts/min total) with 250 ml of Portland cement and approximately 100 ml of water. The block has been exposed to 3 liters of the simulated sea water for more than 1250 hr under conditions of continuous agitation at room temperature. No fissures or rupture are visible in the block, and, activity measurements on the sea water have shown 10 gamma counts/min/ml; that is, less than 0.02% of the total gamma activity has been leached from the block. Two similar blocks are being prepared to verify these results with higher quantities of radioactivity. Special attention will be given to the individual activities, such as cesium, strontium, ruthenium, and the rare earths.

In order to establish the specifications for the block, various ratios of cement, resin, and water and several additives (Bendex, Sta-Dri, and Daraweld) were tried. Most blocks tended to be brittle, and they crumbled after short periods of exposure to the simulated sea water.

Sea disposal of the demineralizer resins by concreting aboard ship would involve sluicing the resins from the demineralizer into a drum, adjusting the volume of water, adding the appropriate amount of cement, mixing, sealing the drum, and dumping it to the ocean. There are, of course, a number of engineering problems which must be studied, the most difficult of which will be the remote handling.

Demineralizer Resin Studies

In order to more fully understand the type of activity which will be sorbed and filtered on the ion-exchange resins in the demineralizer, the laboratory-scale loop shown in Figs. 2.1 and 2.2 was constructed in which to simulate the conditions in the N.S. Savannah system. Information is to be obtained on corrosion products, corrosion rates, release rates, redeposition, effect of corrosion crud on ion-exchange resins, life of demineralizers, sizing of demineralizers, and general reactor water chemistry. The loop will also produce ion-exchange resins exhausted

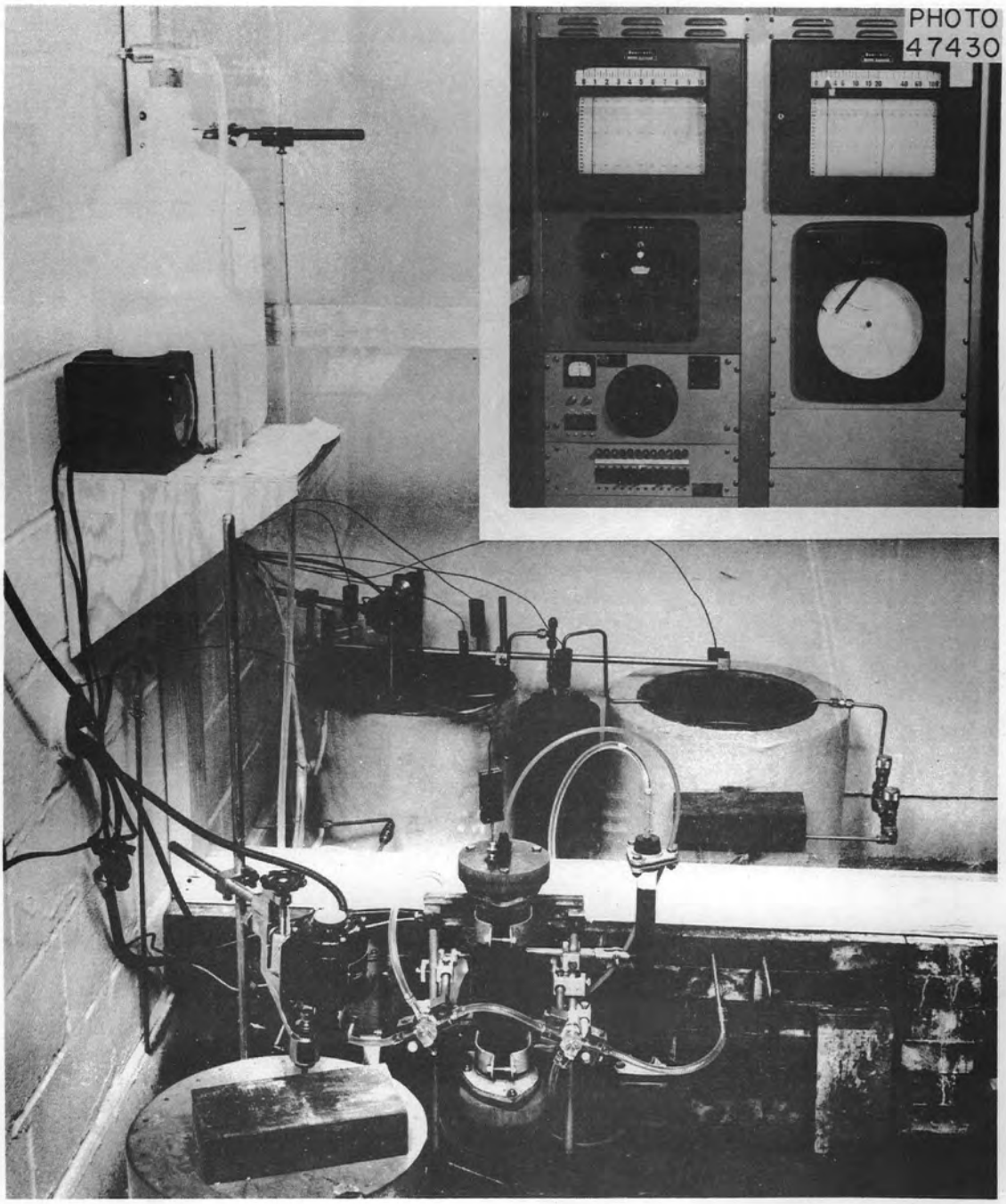

Fig. 2.1. Laboratory-Scale Loop for Studying Demineralizer System Proposed for N.S. Savannah.

UNCLASSIFIED
ORNL-LR-DWG 39870R

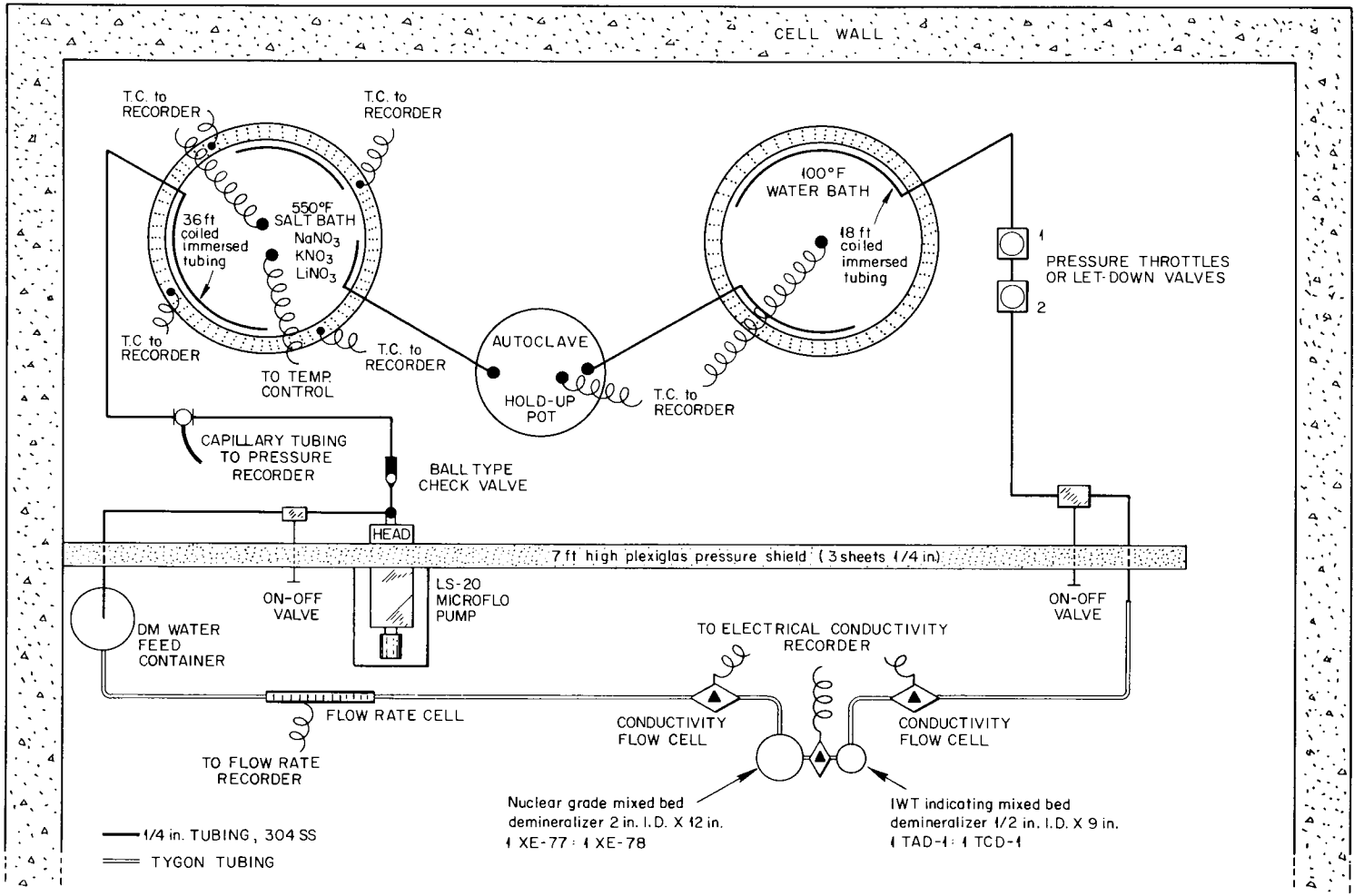

Fig. 2.2. Diagram of Laboratory-Scale Loop for Demineralizer System Studies.

under N.S. Savannah conditions for use in the concreting studies and other disposal techniques.

The demineralized feed water used in the loop is pressurized to 1750 psi with a small pulsating pump, and the pressure is continuously recorded and controlled with a pressure instrument. The water flows through 36 ft of coiled tubing immersed in a $NaNO_3$-KNO_3-$LiNO_3$ salt bath held at 550°F and then moves through a 1-liter, type 304 stainless steel line autoclave into 18 ft of coiled tubing immersed in a water bath at 100°F, which acts as a letdown cooler. From the cooler the water passes through a fine-control, vernier-type, throttling needle valve to reduce the pressure to atmospheric. The water then flows through a conductivity flow cell, an indicating mixed-bed demineralizer, a second conductivity cell, a nuclear-grade demineralizer, a third conductivity cell, and a cell to measure and record the flow rate. Finally, the water is returned to the feed container and again enters the loop cycle. The effects of the process on the system pressure, temperature, electrical conductivity, and flow rate are readily determined by comparison of recorded data.

The loop has been operated for some 1200 hr, both overnight and throughout week-ends without supervision. The operational data have pointed up the need for several changes in the system, including a reduction in tubing diameter to produce velocities which will reduce redeposition and allow the corrosion products to enter the demineralizers. The most important information obtained from loop operation thus far has been the relationship between flow rate, conductivity, and quantity of ion-exchange resin. For a fixed amount of resin, there is an optimum flow rate to produce minimum electrical conductivity, or, conversely, there is an optimum amount of resin for a fixed flow rate to produce minimum conductivity. If high-resistance water is desired, this study points up the need for accurately sizing the demineralizer rather than over-sizing it as a result of conservative estimates. The relationships are being studied more closely in an effort to predict, by extrapolation, the correct sizing of demineralizers to produce ultra pure water.

After necessary revisions of the loop system, the high-temperature portion of the loop is to be irradiated in the ORR reactor. The irradiation will produce active corrosion products which can be easily identified and followed throughout the loop. Thus the information desired from the operation of the loop will be more easily and accurately obtained.

3. PRESSURIZED-WATER IN-PILE TEST LOOP

Design and Construction

Design of the pressurized-water loop described previously[1] was completed, and fabrication and installation of the loop are nearing completion. The design remains basically the same as previously described, with only minor changes. One significant change involves loop temperature control. Originally the water-cooled heat exchanger bypass was to be manually controlled and the loop heaters were to be automatically controlled. It is now evident that better temperature control over a wider range of operating conditions can be achieved best by manual control of the line heaters and automatic control of the heat exchanger bypass.

Installation of the loop is complete except for the in-pile test section; this component is essentially complete. Irradiation tests with dummy fuel specimens are scheduled for a reactor operating cycle beginning early in December, and irradiation tests of fuel specimens are scheduled to start the following reactor cycle.

Shakedown tests on the portion of the loop located within the equipment room were initiated in September. To date only minor difficulties have been encountered, and adjustments are being made as needed. This portion of the loop has been hydrostatically tested at room temperature and 4750 psig in accordance with code standards which will permit loop operation at pressures to 2500 psig and 650°F.

Photographs made during various phases of construction are presented below; they do not represent finished items. Figure 3.1 is a photograph of the loop operating area showing the valve extension handles mounted in the equipment room wall. A portion of the water-sampling station is visible on the right side of this picture. Another view of the operating area and control panel is shown in Fig. 3.2. Figure 3.3 is a photograph of the three Westinghouse type A-150-D main water-circulating pumps. A

---

[1]Maritime Reactor Project Annual Progress Report for Period Ending November 30, 1958, ORNL-2657, p 10.

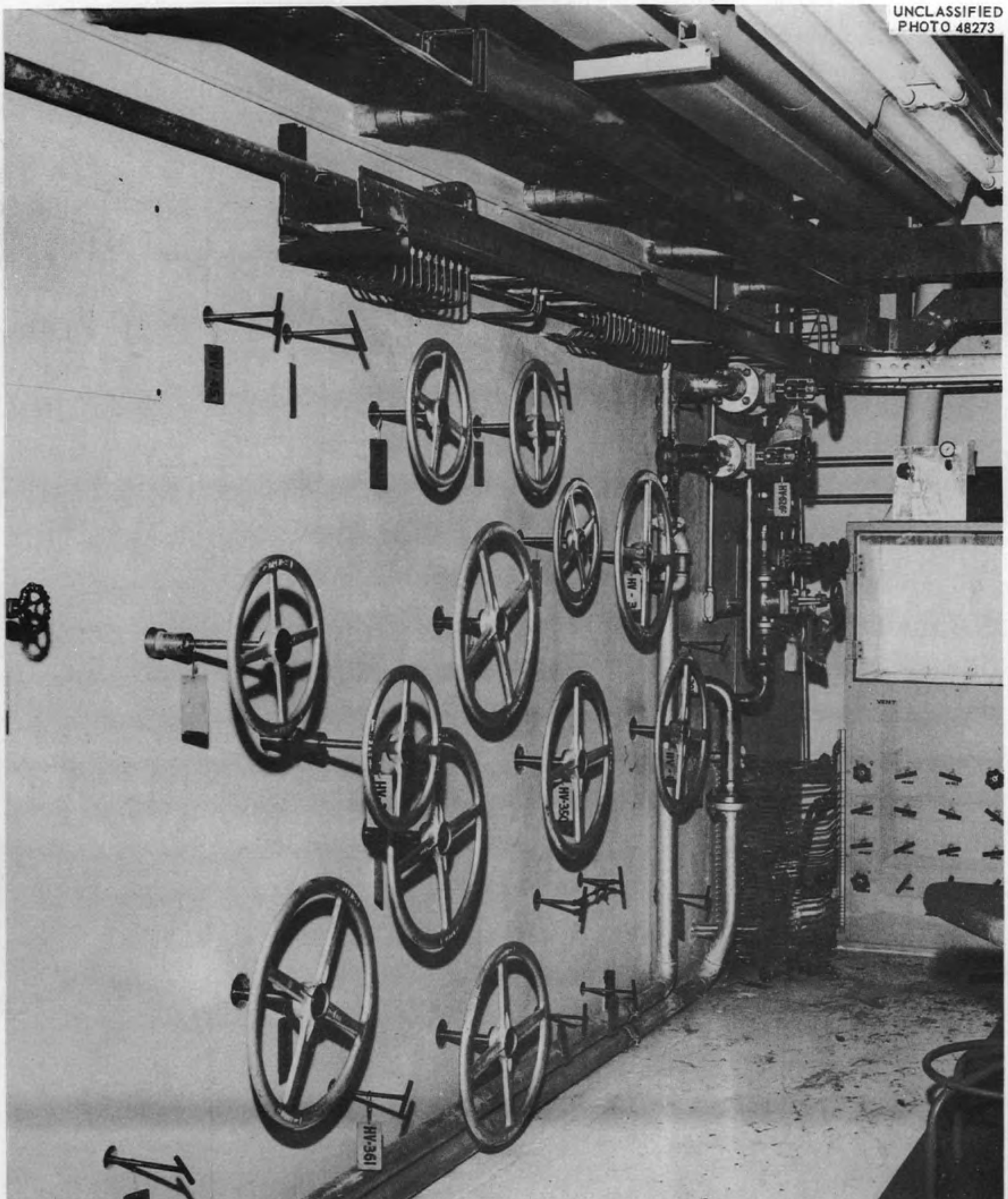

Fig. 3.1. View of Operating Area of ORR Pressurized-Water In-Pile Test Loop.

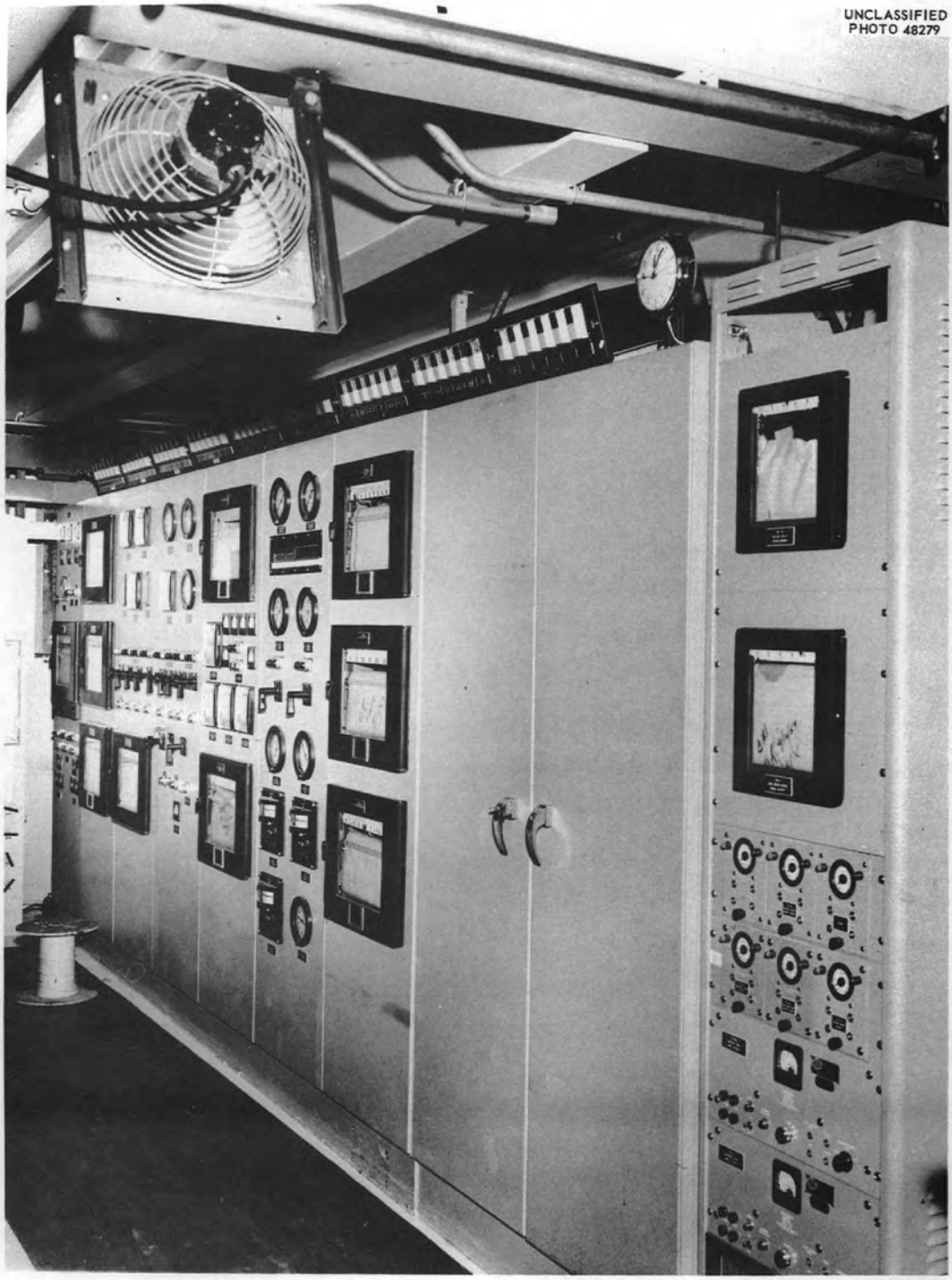

Fig. 3.2. Operating Area and Control Panel of ORR Pressurized-Water In-Pile Loop.

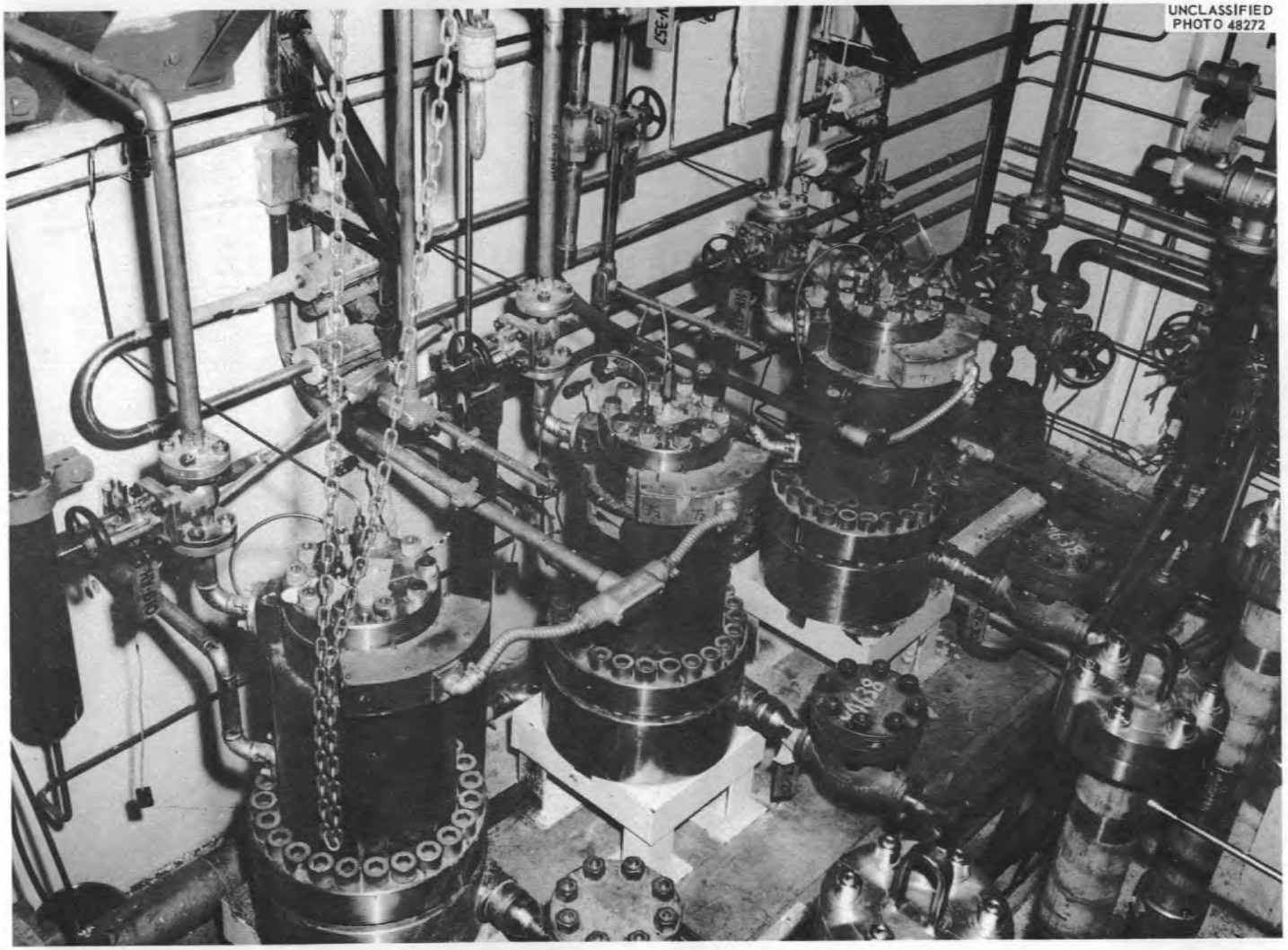

Fig. 3.3. Main Circulating Pumps of ORR Pressurized-Water In-Pile Loop.

portion of the purification system ion-exchange columns may be seen in the lower right corner of this picture. All four of these ion-exchange columns are shown in Fig. 3.4. Lead brick shielding, 4 in. thick, has been stacked around each of these columns since the photograph was made. The water-cooled heat exchanger, consisting of two Griscom-Russell No. C-72 heat exchanger units installed in series, is mounted overhead as shown in Fig. 3.5. Figure 3.6 is a view of the water makeup system which is located outside of the equipment room. The system includes a Milton-Roy feedwater pump, a steam-heated makeup tank, a condensate return pump, two ion-exchange columns, and a drain cooler. Figure 3.7 is a photograph of the pipe trench extending from the equipment room to the pipe chase beneath the pool and is viewed from within the equipment room. The high-pressure lines have been insulated and the trench shielding installed since this photograph was made. The shielding consists of 6 in. of lead brick stacked on top of a 1-in.-thick steel plate. Another 1-in.-thick steel plate covers the lead brick and is flush with the floor. Figure 3.8 is an overall front view of the instrument and control panel. Figure 3.9 is a rear view of the panel shown in Fig. 3.8, and Fig. 3.10 is a rear view of the relay cabinet with the doors open. Figure 3.11 shows the pressure transmitter rack located inside of the equipment room. Figure 3.12 shows the battery-powered motor-generator set and Fig. 3.13 pictures the associated control panel. Figure 3.14 is a view of the portion of the in-pile test section pressure pipes which will be located within the reactor core. The thermocouples shown attached to the outer surfaces will monitor the wall temperature. These pipes will be insulated by a vacuum jacket. Figures 3.15 and 3.16 are views of the in-pile test section assembly. A mockup of a cluster of three fuel pin test specimens and the support assembly may be seen in Fig. 3.16. Figure 3.17 shows the upper end of the in-pile test section. The portion visible in this figure will be located on top of the reactor pressure vessel directly over lattice positions A1 and A2.

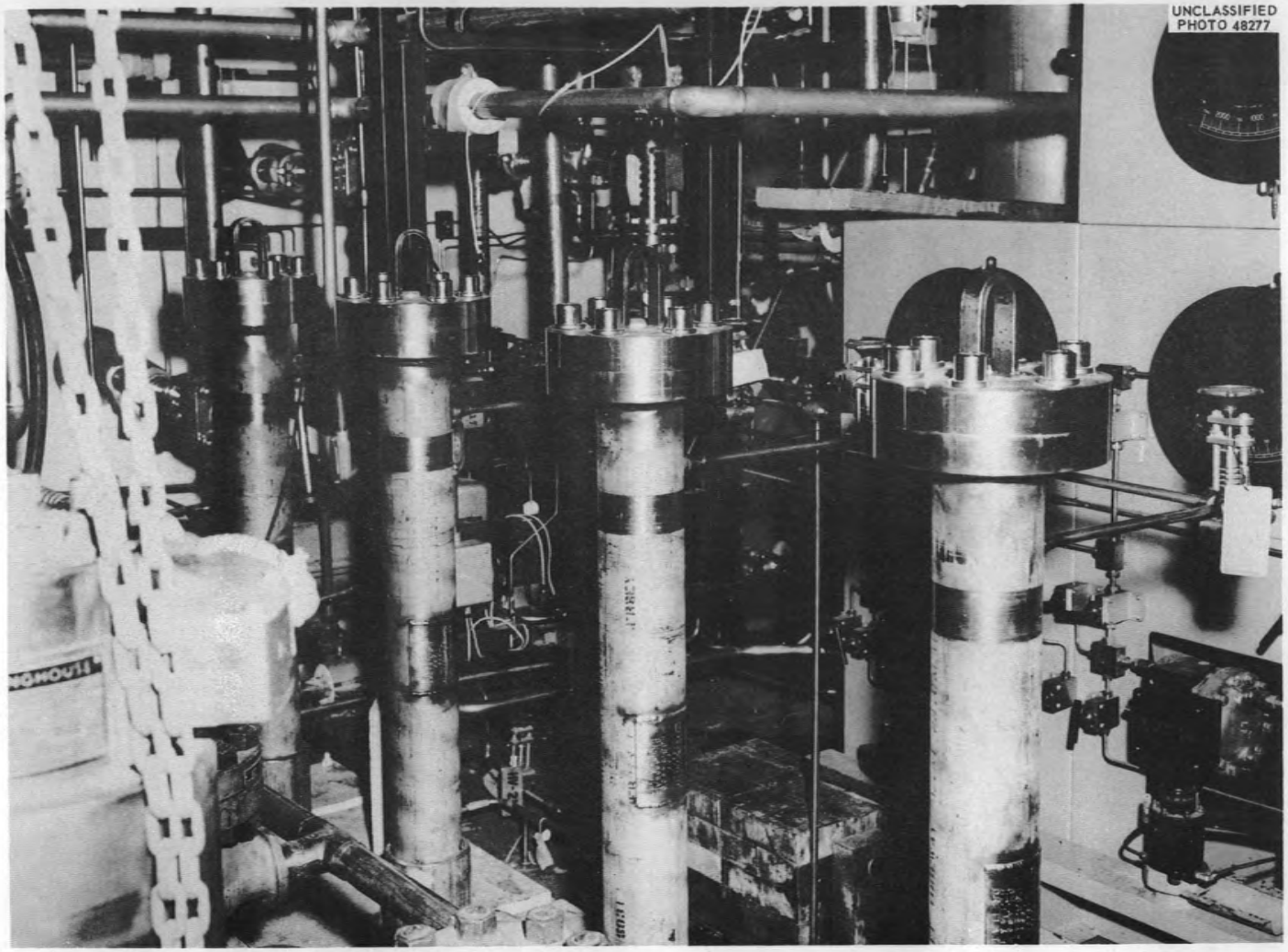

Fig. 3.4. Ion-Exchange Columns of Purification System.

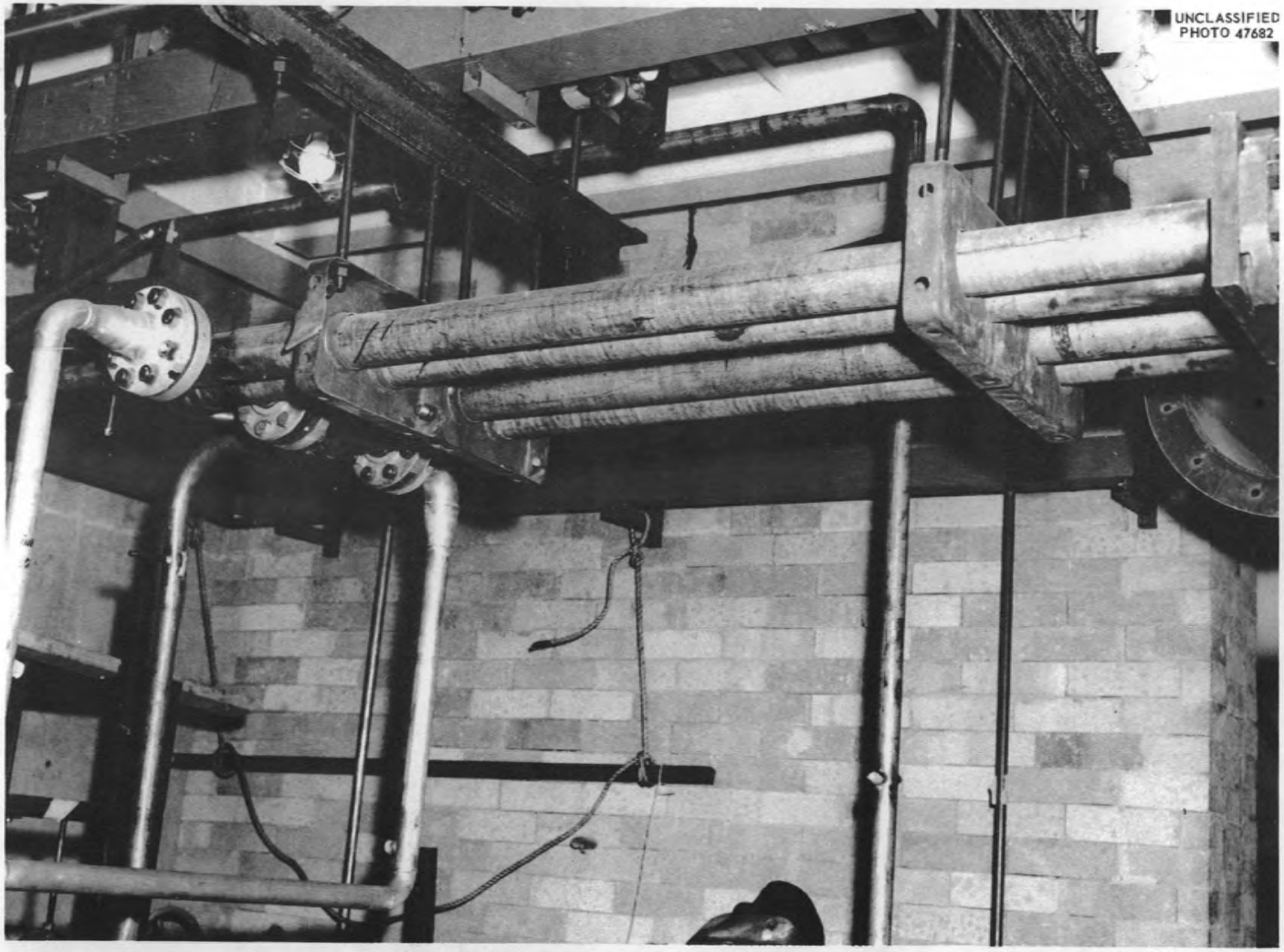

Fig. 3.5. Water-Cooled Heat Exchanger.

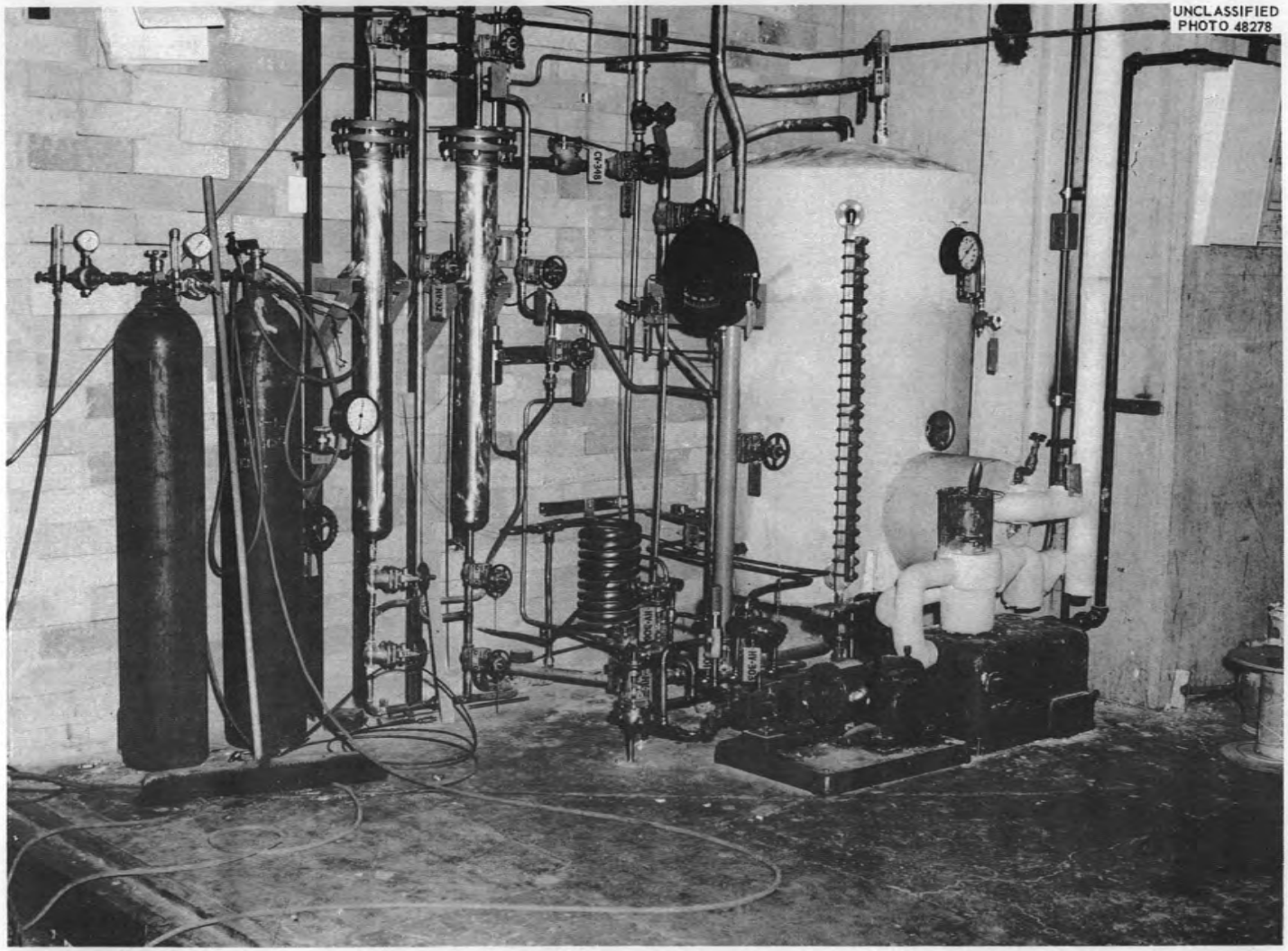

Fig. 3.6. Water Makeup System.

Fig. 3.7. Pipe Trench Extending from Equipment Room.

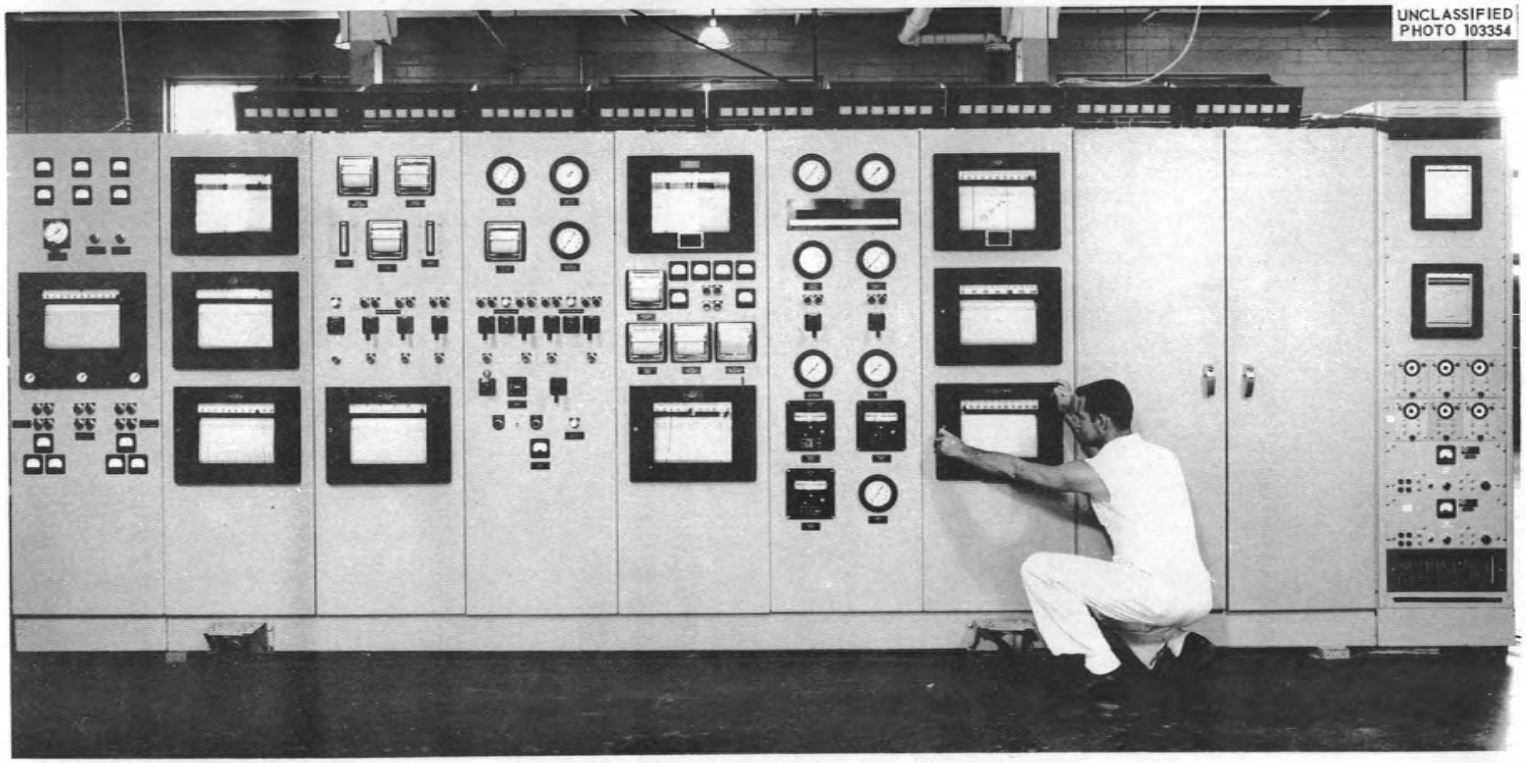

Fig. 3.8. Overall View of Instrument and Control Panel.

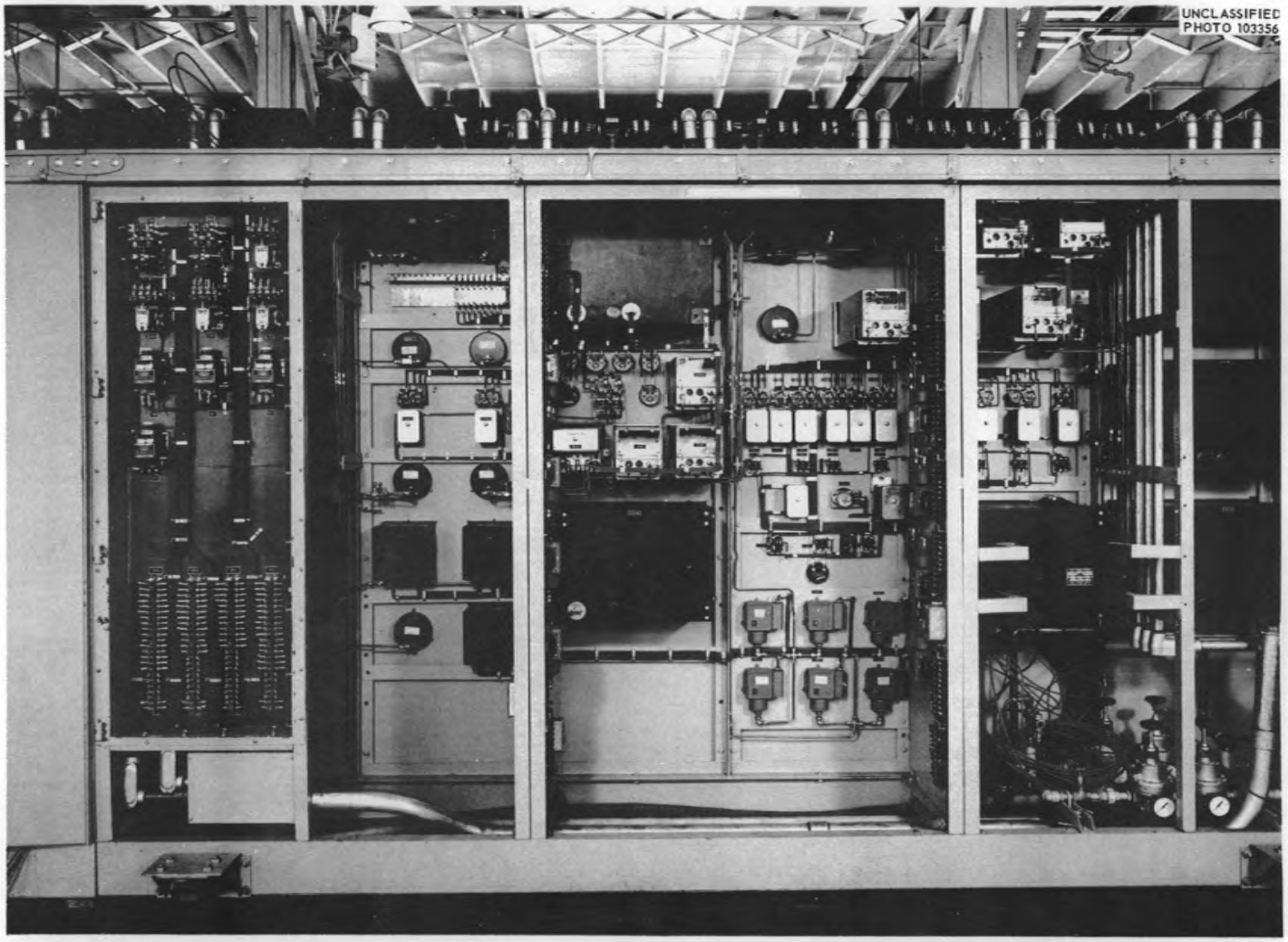

Fig. 3.9. Rear View of Panel Shown in Fig. 3.8.

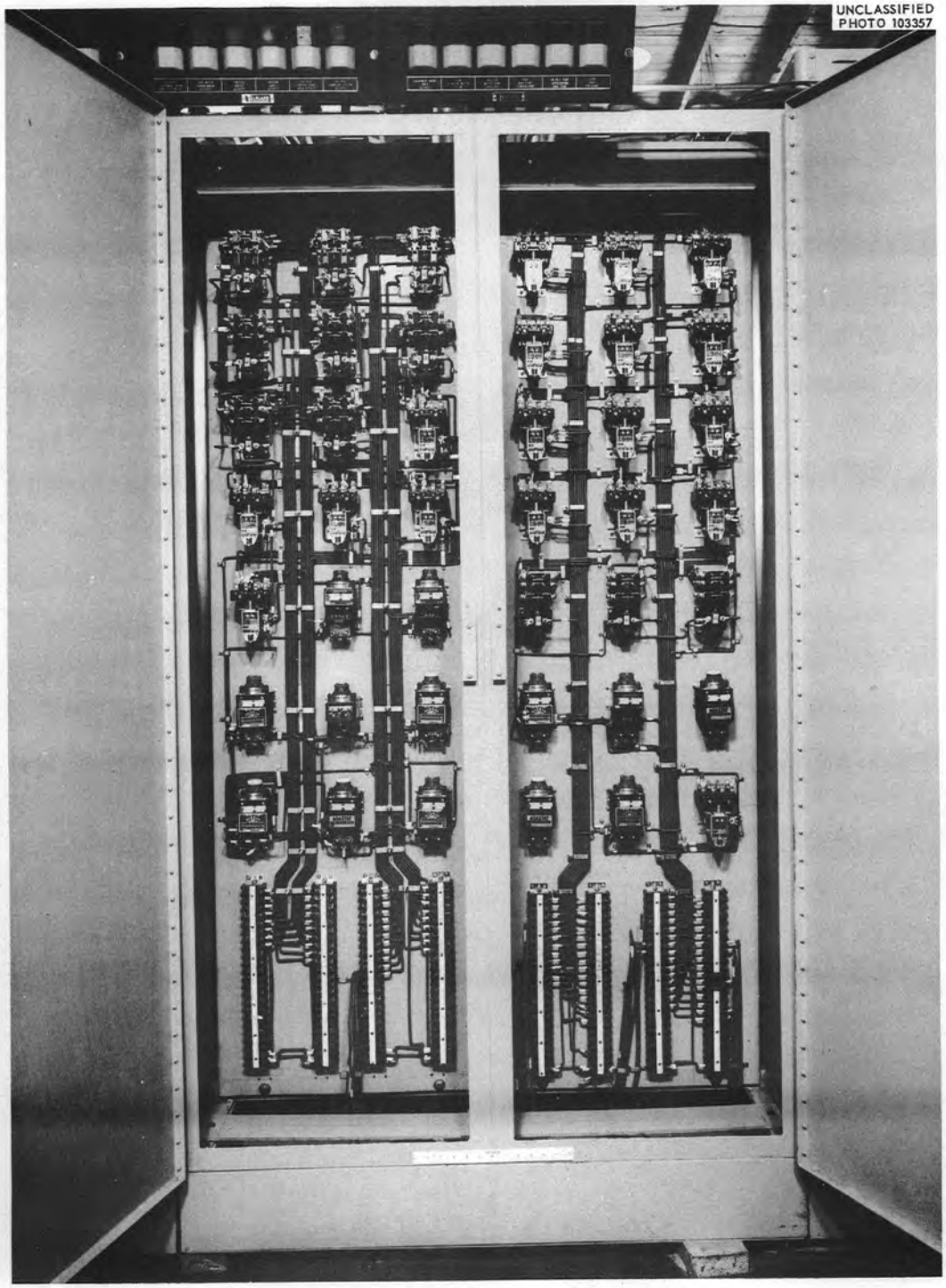

Fig. 3.10. Rear View of Relay Cabinet.

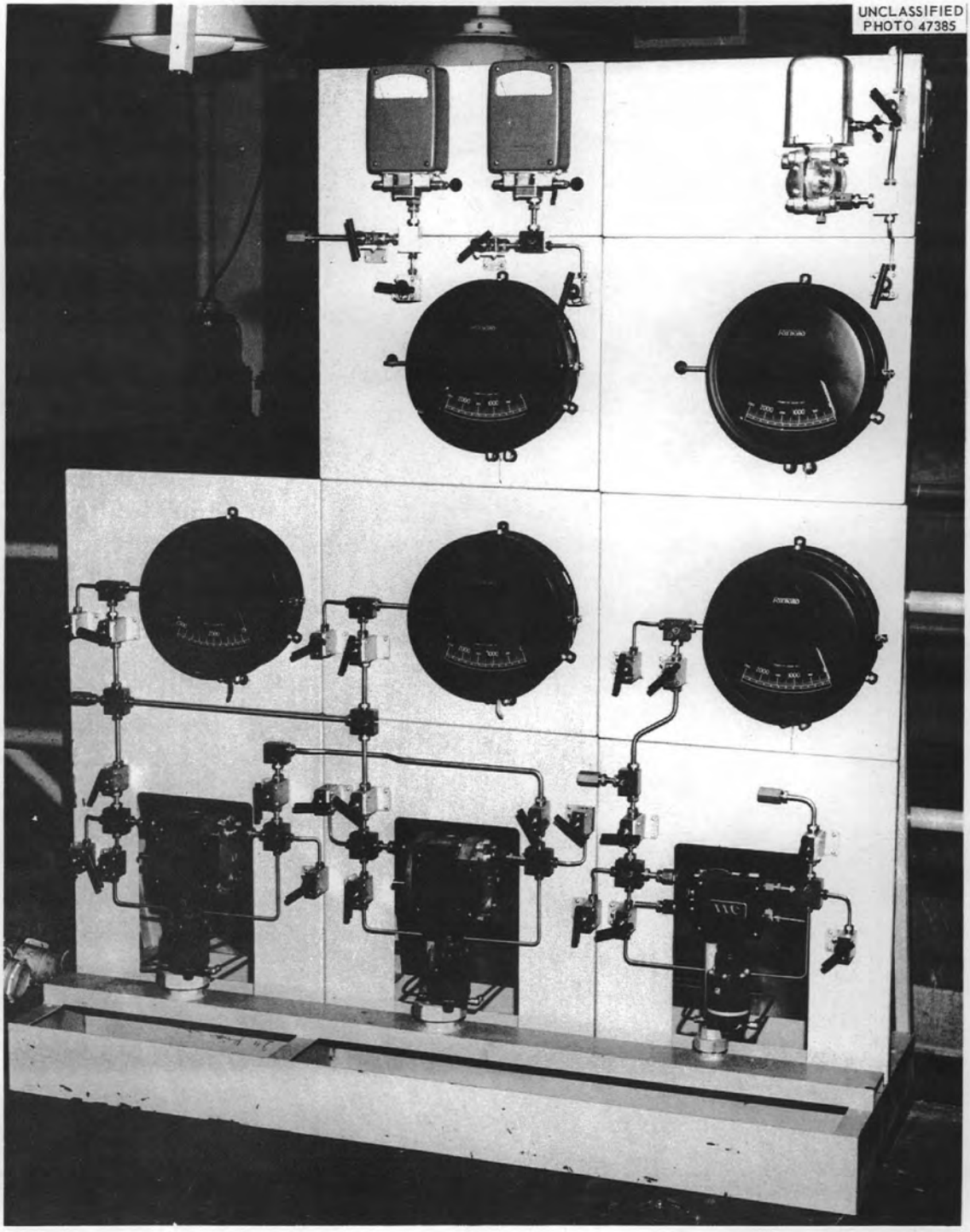

Fig. 3.11. Pressure Transmitter Rack.

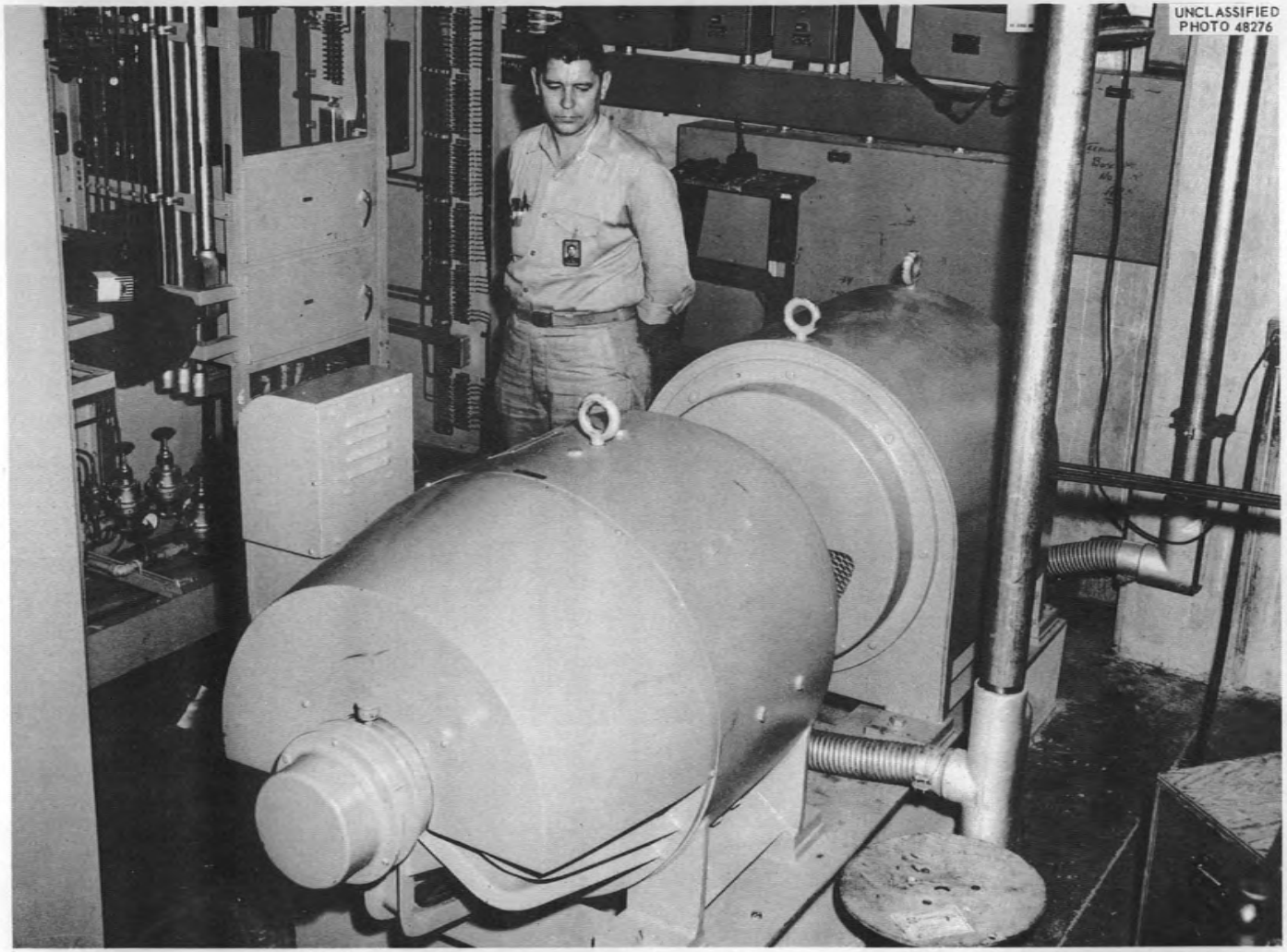

Fig. 3.12. Battery-Powered Motor-Generator Set.

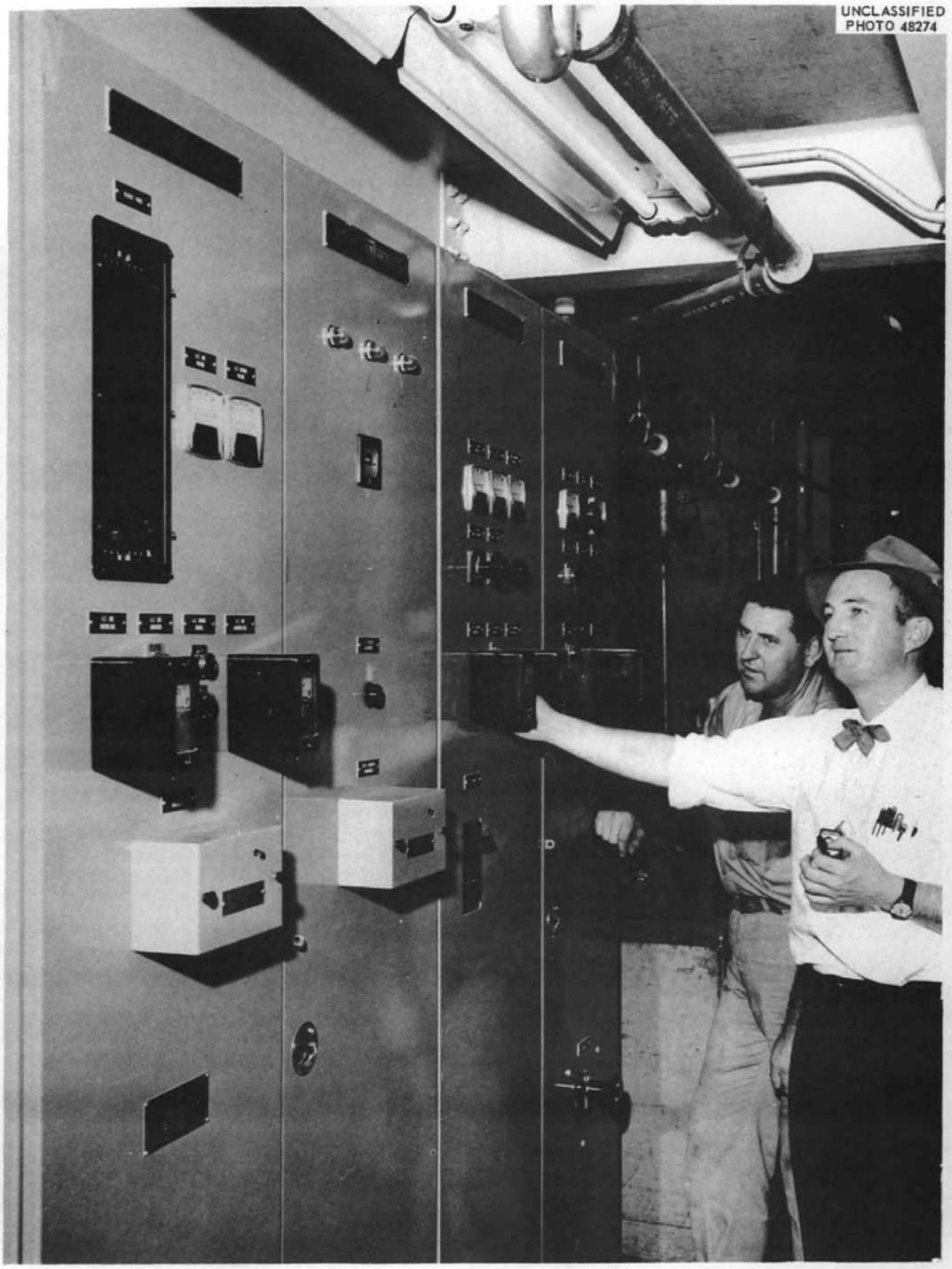

Fig. 3.13. Control Panel for Motor-Generator Set.

UNCLASSIFIED
PHOTO 34647

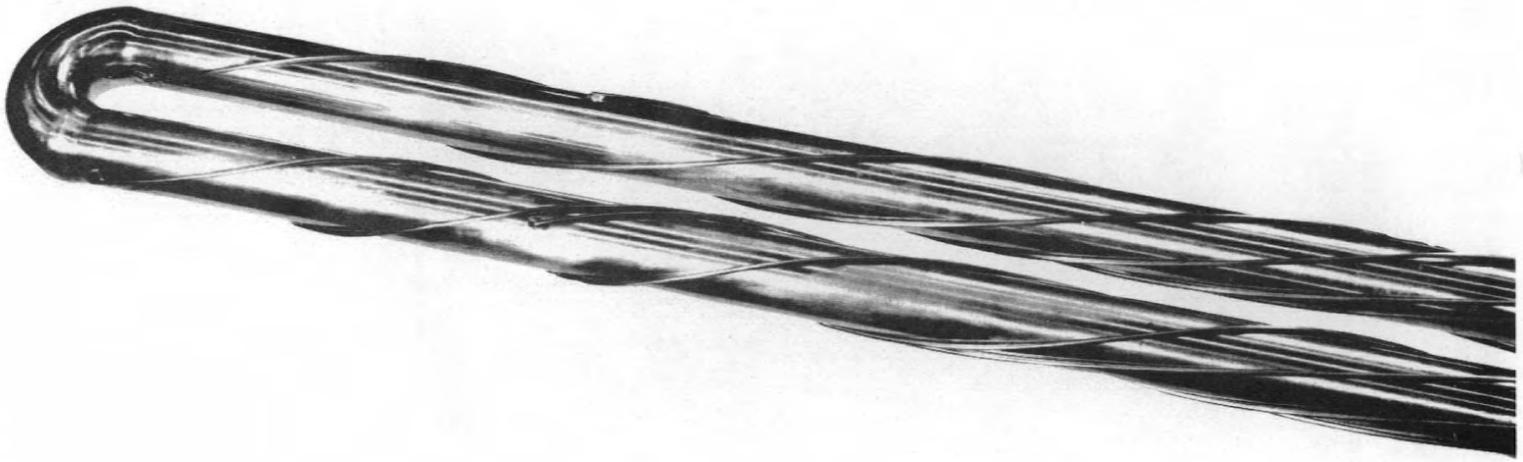

Fig. 3.14. Portion of In-Pile Test Section Pressure Pipes.

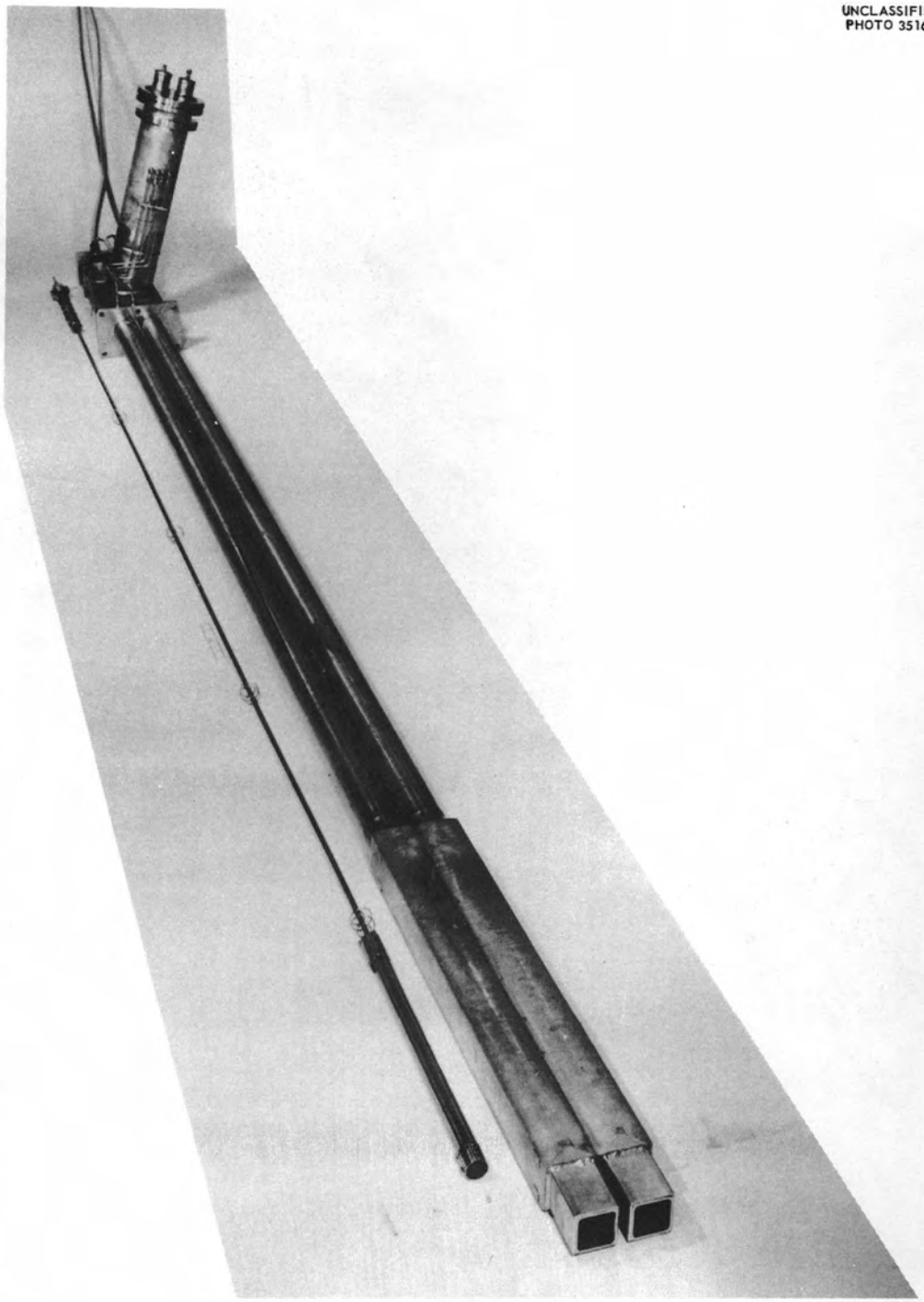

Fig. 3.15. Over-all View of In-Pile Test Section.

UNCLASSIFIED
PHOTO 35159

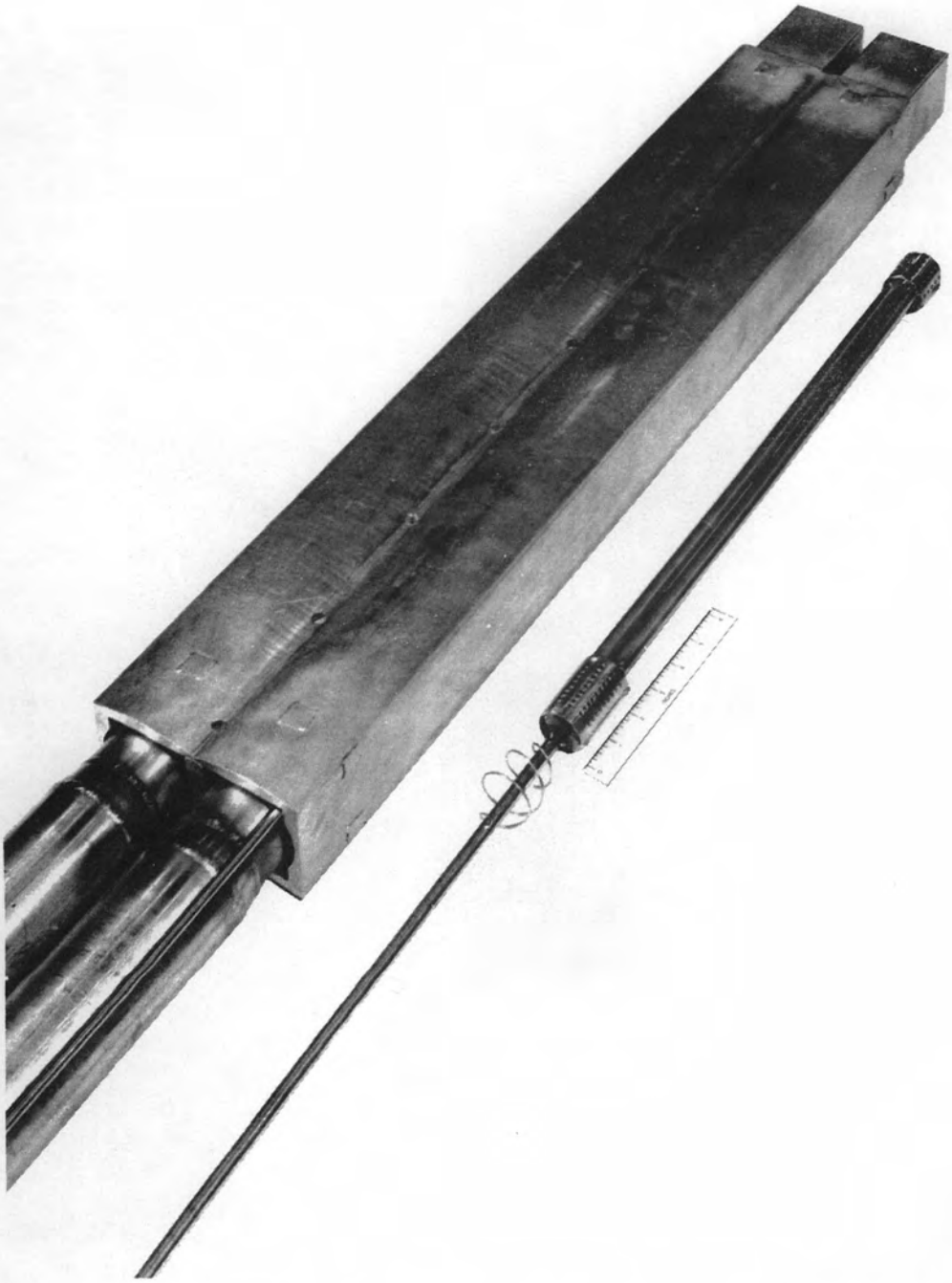

Fig. 3.16. In-Pile Test Section and a Mockup of a Cluster of Three Fuel Pin Test Specimens.

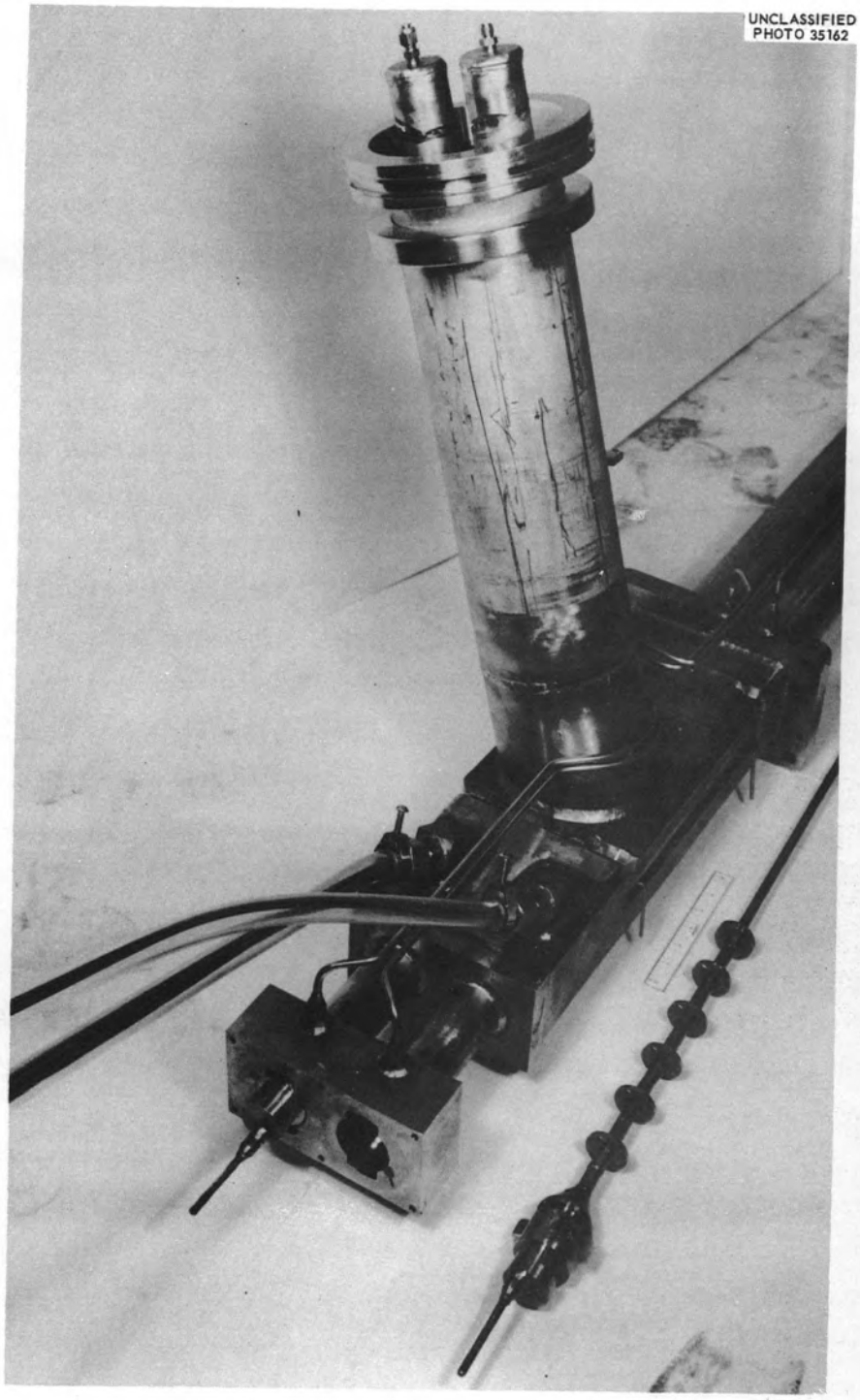

Fig. 3.17. Upper End of In-Pile Test Section That Will Be on Top of Reactor Pressure Vessel.

Flux Measurements

Perturbed flux measurements were made in ORR lattice positions A-1 and A-2 during the routine September intercycle shutdown to obtain the data needed for operation of the pressurized-water loop. The measurements were made with a nuclear mockup of the loop components which duplicated the loop to very close detail, with the exception that the loop water section contained ORR water instead of high-temperature, high-pressure water. Calculations indicate this deviation should alter the determination by less than 2%. Cobalt (100%) wires were used as monitors, and they were activated uncovered and with cadmium covers to obtain information on fast and thermal fluxes. The assembled equipment is shown in Fig. 3.18. A typical specimen mockup is shown in Fig. 3.19. The specimen rods were identical in size (0.5 in. in diameter by 18 in. long) and configuration to typical specimens to be tested (see Fig. 3.16). They contained 3% enriched UO_2 pellets of approximately 95% theoretical density, and a set of segmented rods was simulated by the insertion of stainless steel plugs at two locations in each rod. Monitor wires were located as indicated in Fig. 3.20. The monitor wires were activated by operating the ORR at a constant low power level for 1 hr. Simultaneously another monitor was irradiated in an ORR hydraulic tube to obtain a relative measurement of the ORR power level. The monitor wires were subsequently cut into 1-in. segments, weighed, and gamma counted to obtain activities which could be related to neutron flux at the various positions.

Conversion of the monitor activities into flux values and a subsequent weighting of the fluxes as indicated by the wires associated with the respective rods yielded the curves of Fig. 3.21. These curves may be expected to change in shape and magnitude during a reactor cycle because of control rod withdrawal and fuel burnup. An increase in the maximum flux of up to 12% would be expected because of fuel burnup, but withdrawal of the control rods will decrease this maximum to some extent and make the flux distribution more uniform. Inspection of the axial

UNCLASSIFIED
PHOTO 34920

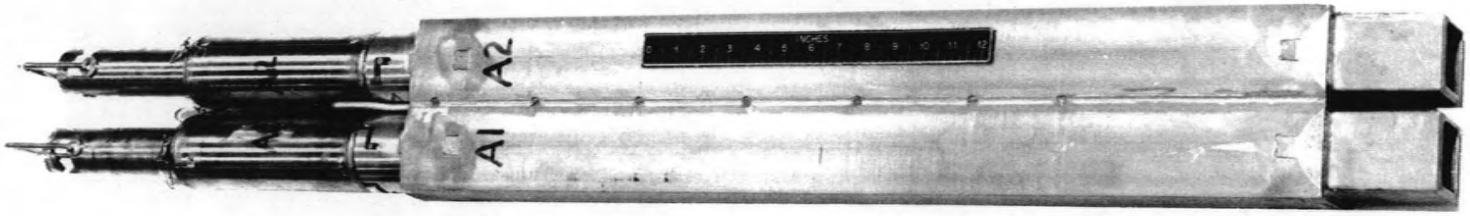

Fig. 3.18. Equipment for Flux Measurements in ORR Lattice Positions A-1 and A-2.

UNCLASSIFIED
PHOTO 34998

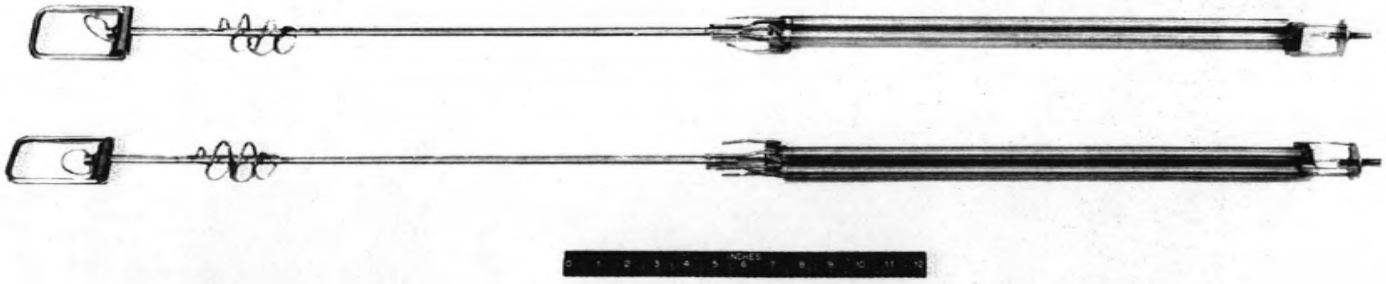

Fig. 3.19. Fuel Specimen Mockup for Flux Measurements.

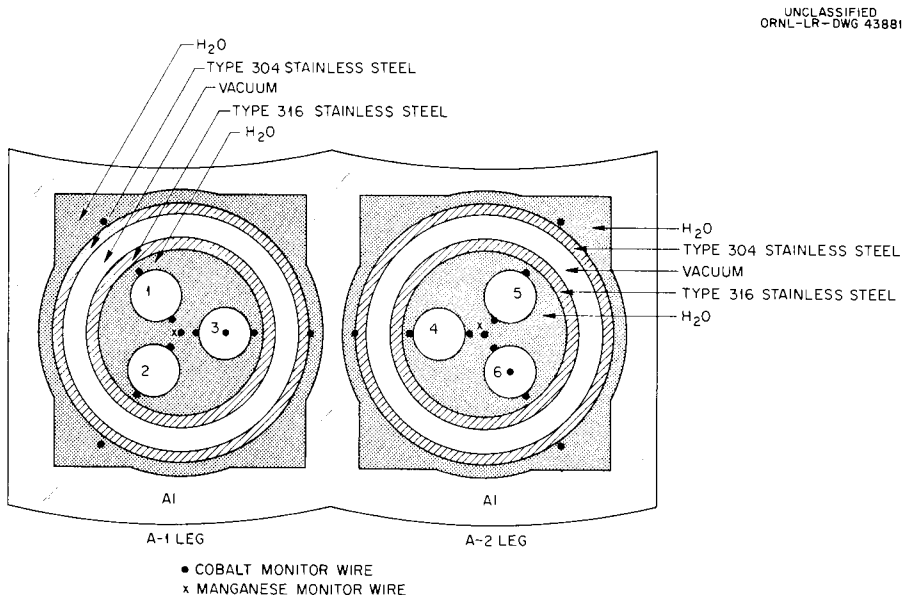

Fig. 3.20. Fuel Rod Orientation and Location of Flux Monitor Wires.

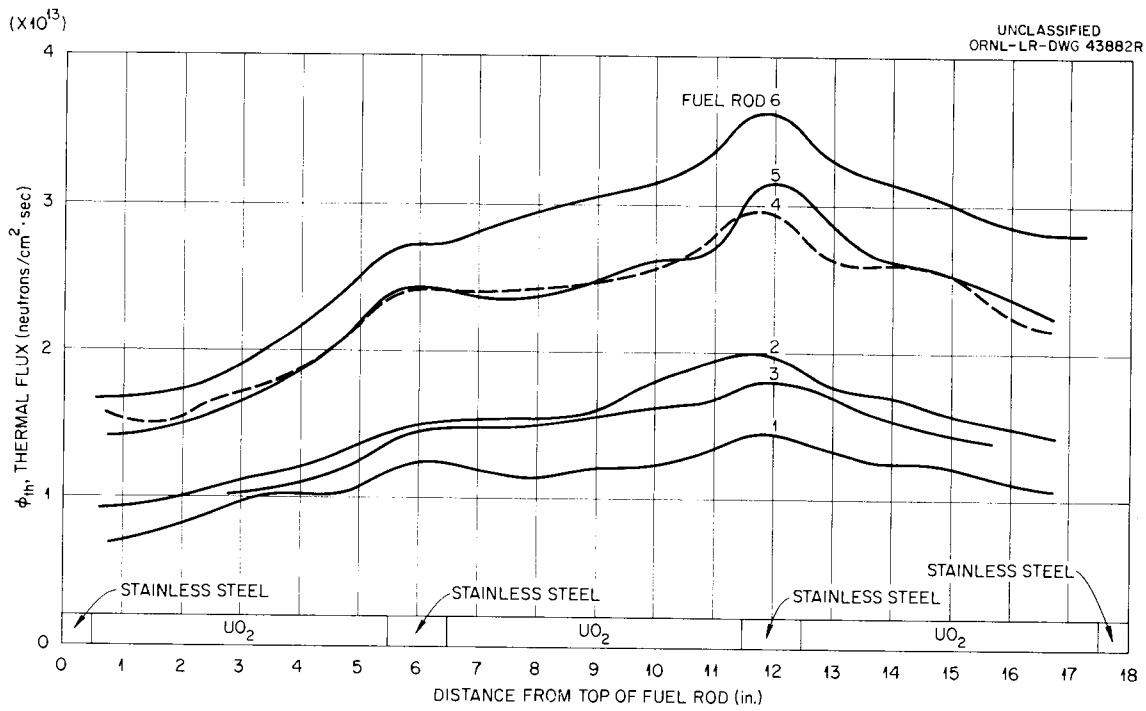

Fig. 3.21. Thermal Flux vs Axial Position Extrapolated to Operation at 20 Mw from Measurements at 1.3 kw with a Newly Refueled ORR Core and the Control Rods 15 in. Out.

variation of the thermal flux indicates local peaking of the flux in the rods caused by the decreased depression of the flux in the stainless steel relative to the fuel. These peaks will not occur in rods fueled throughout their entire length. Typical relative peak values of the thermal flux relative to the flux in the lowest flux rod (No. 1) are given below.

Fuel Rod	Ratio of Maximum Flux Values in Each Rod to Flux in Rod 1
1	1.0
2	1.4
3	1.3
4	2.1
5	2.3
6	2.6

Actual test specimens will probably not contain 3% enriched uranium. Thus the variations in flux from the measured values as a function of enrichment will be obtained from results of cell calculations using the SNG-S4 code. A plot of the extrapolation factor is presented in Fig. 3.22.

Aluminum wire with 0.15% manganese content was used to obtain a confirmatory check of the cobalt flux measurement by simultaneous exposure at the central location of each leg of the loop. In the A-2 position the agreement between the two methods was very good, there being about 5% difference. In the A-1 position the difference was about 20%. An analytical study is under way to determine the confidence to be placed in calculated techniques in lieu of actual flux measurements.

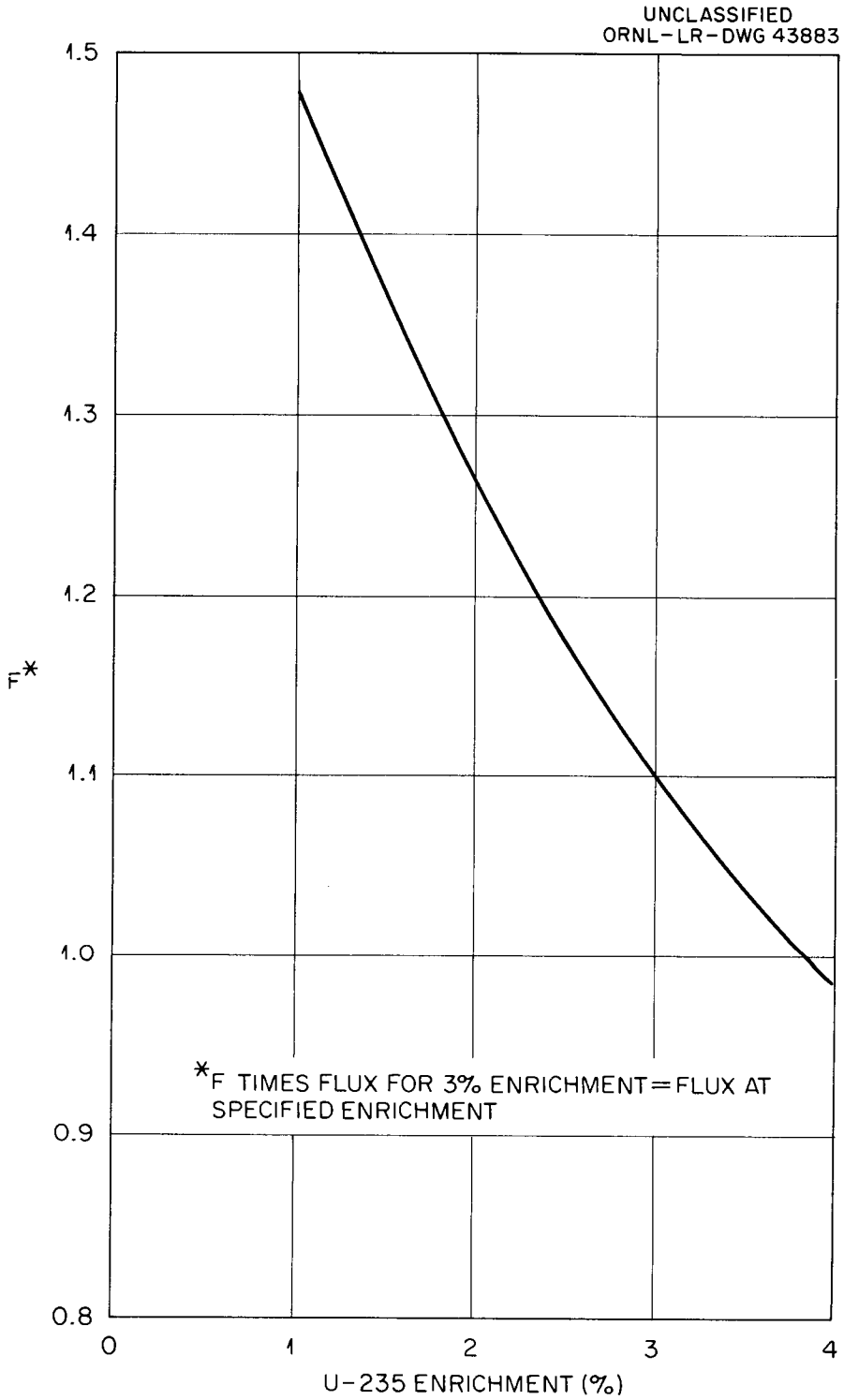

Fig. 3.22. Extrapolation Factor vs Enrichment.

4. METALLURGY

Rotary Swaging of Stainless Steel-Clad UO_2 Fuel Rods

The rotary swaging process is being investigated as a means for fabricating stainless steel-clad UO_2 fuel rods. With the swaging technique it is possible to simultaneously clad and compact UO_2 into high-quality fuel rods. The swaging process also results in substantial reductions in cost compared with the presently used process in which the UO_2 pellets are cold pressed and sintered to form the fuel rod. Initial studies[1] with three basic types of UO_2 (ceramic, fused, and high fired) have indicated that oxide densities as high as 90% of theoretical can be achieved by swaging at room temperature.

Effect of Type of Oxide Density

The densities achieved by swaging three types of UO_2 at room temperature in 0.750-in.-OD, 0.035-in.-wall, type 304 stainless steel tubing to a total reduction in area of approximately 55% are listed in Table 4.1. At this reduction, the fused-and-ground material swaged to the highest density (87 to 91% of theoretical). The high-fired oxide swaged to a somewhat lower range of densities and the ceramic-grade oxide, which is generally used for producing cold-pressed and sintered pellets, swaged to much lower densities. From this series of studies, it may be stated that, in general, the swageable grades of UO_2 are characterized by low surface area and high tapped bulk density.

Effect of Swaging Temperature on Oxide Properties

It was found that the density to which an oxide would swage could be significantly increased by fabrication of elevated temperatures and that the magnitude of the density increase was dependent on the working temperature. This effect is illustrated in Fig. 4.1, which shows that

---

[1]J. T. Lamartine and W. C. Thurber, Development of Swaged Stainless Steel Fuel Rods Containing UO_2, ORNL CF-59-10-8 (Oct. 12, 1959).

Table 4.1. As-Swaged Densities of Various Types of UO_2 at 55% Reduction in Area

Type of Oxide	Surface Area (m^2/g)	Tapped Bulk Density (g/cm^3)	Cold-Swaged Density (% of theoretical)
Ceramic	0.4 to 5.5	2.1 to 5.0	53 to 76
High fired	0.02 to 0.8	3.1 to 6.2	80 to 88
Fused and ground	0.02 to 0.1	5.0 to 6.4	87 to 91

the maximum density of high-fired, microatomized oxide was increased from 85% of theoretical with room-temperature swaging to about 92% of theoretical by swaging at 800°C. It may also be seen in Fig. 4.1 that 800°C represents an optimum swaging temperature, with lower densities being produced at working temperatures greater than or less than 800°C. In addition to affecting oxide density, swaging at elevated temperatures promotes changes in the ratio of oxygen to uranium in the oxide. As shown in Fig. 4.2, the ratio of oxygen to uranium in high-fired, microatomized UO_2 decreased with increasing swaging temperature, and near-stoichiometric proportions were attained at about 1000°C. Calculations indicate that the free energies of formation of chromium oxide and UO_{2+x} at 800°C are such that the chromium in the cladding could reduce non-stoichiometric UO_2.

The data of Fig. 4.3 show that swaging UO_2 at high temperatures results in a reduction in surface area with increasing total rod swaging reduction. Metallographic examination of hot-swaged UO_2 has indicated that this decrease in surface area is due to actual bonding of oxide particles during swaging. Since the surface area of cold-swaged oxide increases with reduction, as shown in Fig. 4.3, it is thought that the oxide particles are fragmented during cold swaging and that densification under these circumstances is merely the result of mechanical compaction. These observations suggest that fission-gas retention may be superior with hot-swaged oxides.

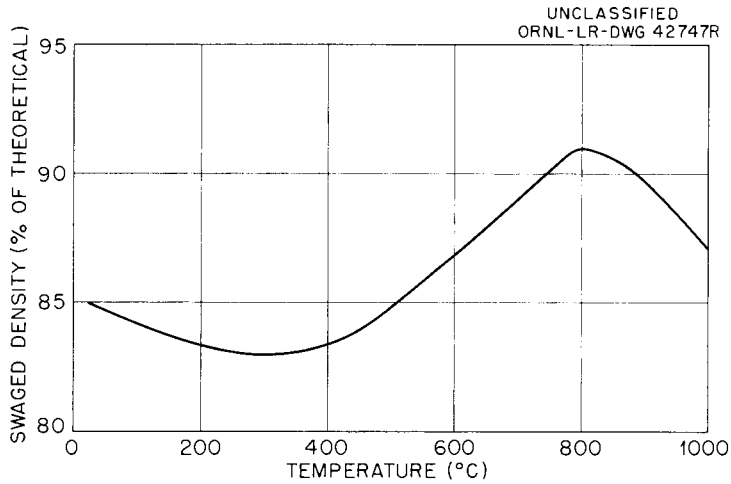

Fig. 4.1. Effect of Swaging Temperature on the Characteristic Density of High-Fired Microatomized UO_2 (SR-772). Reduction in area approximately 69%.

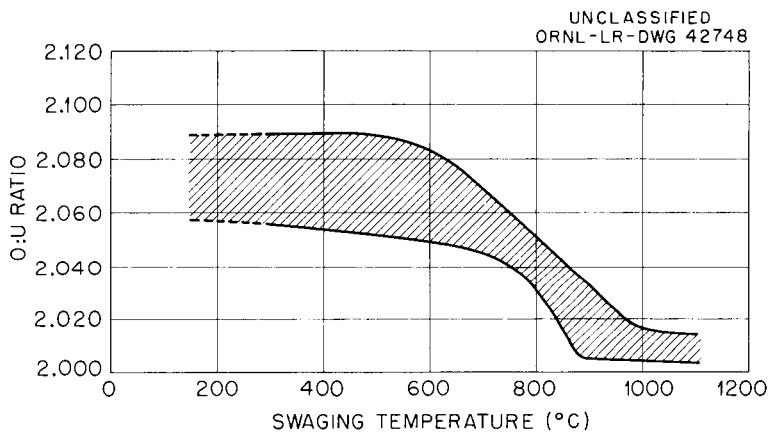

Fig. 4.2. Effect of Swaging Temperature on the O/U Ratio of Oxygen to Uranium in High-Fired Microatomized UO_2 (SR-772).

Evaluation of Commercially Produced Swageable Grades of UO_2

Swageable grades of UO_2 have been procured from three different vendors and evaluated. Properties of the as-received powders are listed in Table 4.2. The densities obtained with each of these materials after swaging to 55% reduction in area at room temperature and at 800°C are listed in Table 4.3.

Table 4.2. Properties of As-Received Swageable Grades of Commercially Produced UO_2

Oxide Identification	General Type	Tapped Bulk Density (g/cm^3)	Surface Area (m^2/g)	Oxygen-to-Uranium Ratio	Particle Size
A	High fired	5.89	0.067	2.012	-80 mesh
B	Fused and ground	6.45	0.05	2.026	-20 mesh
C	High fired	5.00	0.02	2.041	-100 +325 mesh

Table 4.3. As-Swaged Densities Obtained with Commercial Oxides At Approximately 55% Reduction in Area

Oxide Identification	Actual Reduction In Area (%)	As-Swaged Density (% of theoretical)	Swaging Temperature (°C)	As-Swaged Surface Area (m^2/g)
A	55.2	85.9	~ 25	0.52
	55.9	90.7	800	0.22
B	55.1	89.6	~ 25	0.37
	55.8	93.2	800	0.09
C	54.9	88.3	~ 25	0.24
	55.8	86.6	800	0.05

Fabrication of Swaged Rods Into Fuel Bundle

A 16-rod fuel bundle in a 4-by-4 array has been fabricated from swaged rods and assembled by brazing with electroless nickel. The type 304 stainless steel rods, which contained alumina powder to simulate UO_2, were cold swaged from 0.750 in. OD to 0.500 in. OD in four passes. The alumina powder was held in place during swaging by specially designed end plugs that also served as final end closures for the finished rods. Rod-to-rod reproducibility after swaging was as follows:

Length	38.467 ± 0.188 in.
Diameter	0.500 ± 0.005 in.
Weight of alumina charge	308 ± 2 g

The rods were all cut to a uniform length of 38 9/32 in. by machining excess metal from the solid portion of the end plugs, assembled in a brazing jig with electroless-nickel-plated ferrule spacers, and brazed at 1010°C for 1/2 hr in hydrogen. Examination of the brazed bundle showed that all rods were firmly joined to the spacer ferrules. There was no distortion or other adverse affects as a result of the rod having been initially severely cold worked. Interrod spacing, bow, and squareness measurements were made on the bundle and are summarized in Table 4.4. Differences in the interrod spacing dimension are thought to be due to uneven jig pressure between sides of the bundle and can be easily corrected by using a more suitable jigging arrangement. The bundle is shown in Fig. 4.4.

Swaging of Small-Diameter Rods

To determine the adaptability of swaging to the production of thin-walled fuel rods of small cross section, several small-diameter rods were swaged and evaluated. One 0.100-in.-OD, 0.010-in.-wall, type 347 stainless steel tube and two 0.187-in.-OD, 0.010-in.-wall, type 304 stainless steel tubes were filled with -100 +325 mesh high-fired UO_2 and cold swaged to approximately 55% reduction in area. The tube ends were

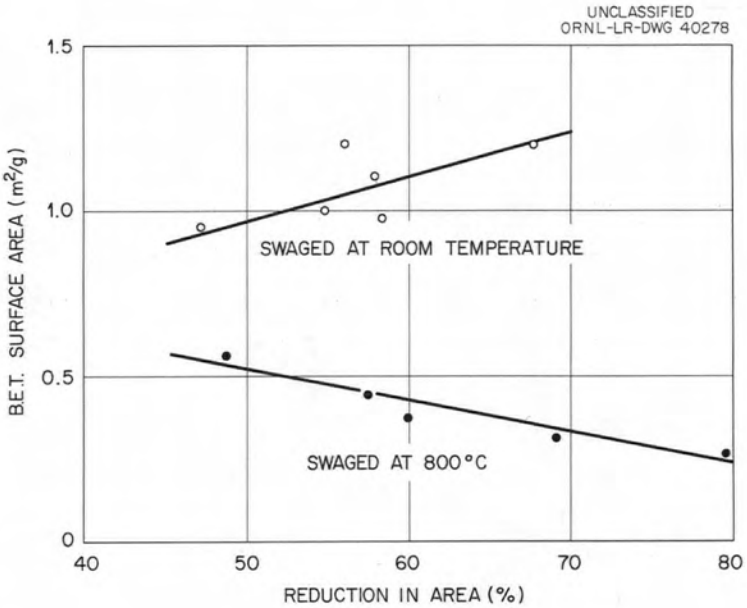

Fig. 4.3. Surface Area of UO_2 (SR-772) As a Function of Total Rod Swaging Reduction.

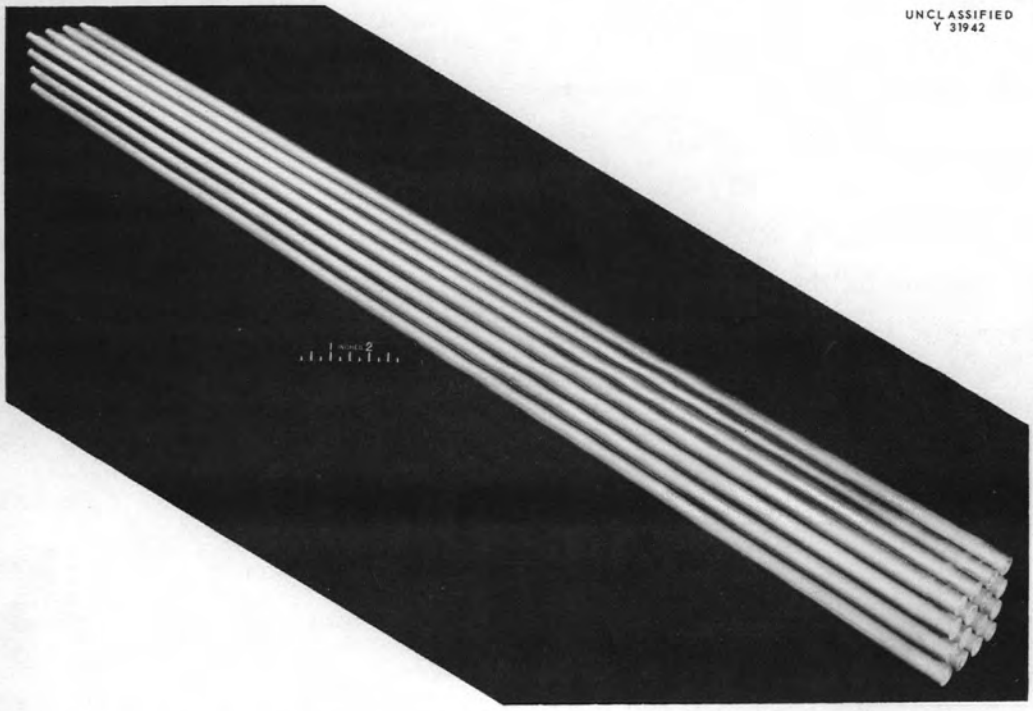

Fig. 4.4. Fuel Bundle Assembled from Swaged Rods by Hydrogen Brazing.

closed by crimping and welding. The UO_2 densities achieved in the three capsules are indicated in Table 4.5.

Table 4.4. Dimensions of Brazed Fuel Bundle Containing Cold-Swaged Rods

	Side A	Side B	Side C	Side D
Average interrod spacing, in.	$0.100^{+0.015}_{-0.025}$	$0.103^{+0.012}_{-0.018}$		
Maximum bow, in.	+0.020	+0.018	+0.023	-0.023
Squareness (deviation from 90°)	±0.5	±0.5	±0.75	±1.0

Table 4.5. Density of UO_2 Swaged in Small-Diameter, Thin-Walled Tubes

Capsule and Oxide Identification	Capsule Outside Diameter (in.)		As-Swaged Wall Thickness (in.)	Actual Reduction in Area (%)	As-Swaged Density (% of theoretical)
	Initially	As-Swaged			
A	0.100	0.071	0.011	50.0	93.5
B	0.187	0.123	0.009	57.1	89.8
C	0.187	0.1235	0.010	56.5	90.8

As may be seen from the data of Table 4.5, the 0.100-in.-OD tube (capsule A) swaged to the highest density, that is, 93.5% of theoretical at 50% reduction in area. Capsules B and C, which were swaged to somewhat higher reductions, had slightly lower oxide densities. The oxide densities in all three of the capsules were 2 to 5% higher than achieved with the same oxide when swaged in 0.750-in.-OD tubes to comparable reductions.

During fabrication capsule B developed an axial crack about 2 in. long and some UO_2 was lost. The loss of oxide may account for the relatively low density of the material in this capsule. Metallographic

examination of cross sections of the three capsules revealed additional cracks on the inner wall of capsule B that were about 0.003 in. deep and cracks in tube C that were about 0.004 in. deep. No cracks were noted in the wall of tube A. The wall cracks in capsule C are shown in Fig. 4.5.

Swaging Fuel Tubes Clad Internally and Externally

The feasibility of producing annular, internally and externally clad, fuel tubes by swaging is also being investigated. As working criteria, it was stipulated that an annular-tube fuel bundle would have the same area of UO_2 and area of stainless steel per fuel channel as is used in Core I of the N.S. Savannah reactor. Although several bundle configurations satisfy these criteria, a configuration consisting of an 8-by-8 array of rods each having an outer sheath diameter of 0.864 in. and an inner sheath diameter of 0.397 in. was selected as being most practical for study. Work to date has been mainly concerned with swaging annular type 304 stainless steel capsules containing alumina (to simulate UO_2) to these dimensions without using a mandrel to control the inner sheath geometry. Cross sections of three such capsules are shown in Fig. 4.6. The initial outer and inner tube diameters of each of the capsules were 1.250 and 0.750 in., respectively. The initial tube wall thickness in each case was 0.035 in. It may be seen in Fig. 4.6 that the degree of inner tube distortion was somewhat dependent on the reduction schedule. Tube No. 1, which received a total reduction in cross-sectional area of 36.9% at about 9% reduction per pass, shows a high degree of inner sheath wrinkling. Tube No. 2, however, which was reduced 37.6% in area at about 5% per pass, shows practically no inner tube distortion. Although tube No. 3 was reduced 44.2% at 5% per pass, inner tube wrinkling was not as great as in tube No. 1. One capsule containing UO_2 has been swaged to a total reduction in area of 53.1% with a minimum of inner sheath wrinkling. The oxide density achieved with this capsule was about 7% less than that obtained within a solid rod swaged to a similar reduction.

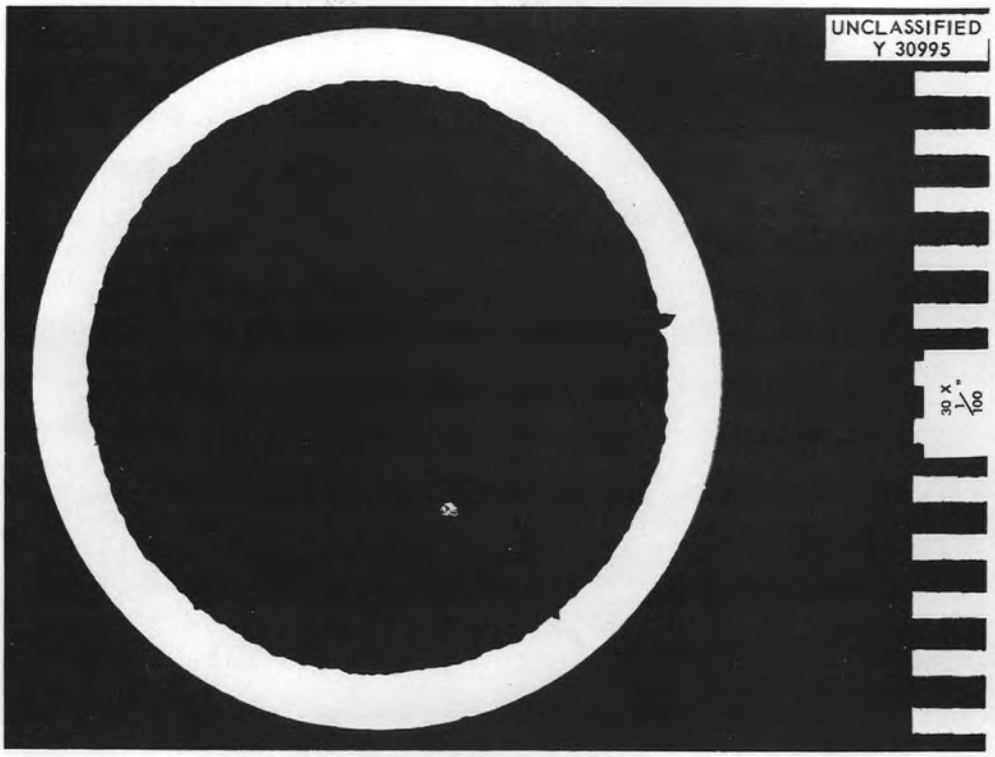

Fig. 4.5. Cross Section of 0.187-in.-OD Type 347 Stainless Steel Tube (Capsule C) Cold Swaged to Reduction in Area of 56.5%. Note tube-wall cracks. As-polished. 30X.

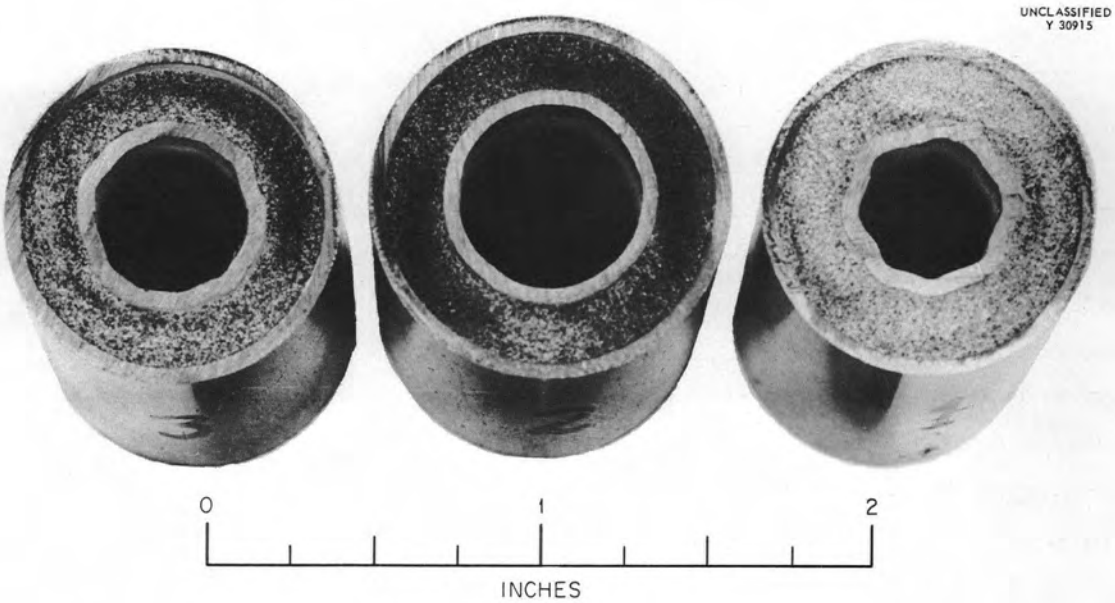

Fig. 4.6. Cross Sections of Swaged Tubular Fuel Capsules.

Compartmented Fuel Plate Development

Compartmented fuel plates containing bulk UO_2 fuel bodies offer several significant advantages over the more conventional rod designs presently employed in most pressurized-water reactors.[2] The flat-plate concept is illustrated in Fig. 4.7.

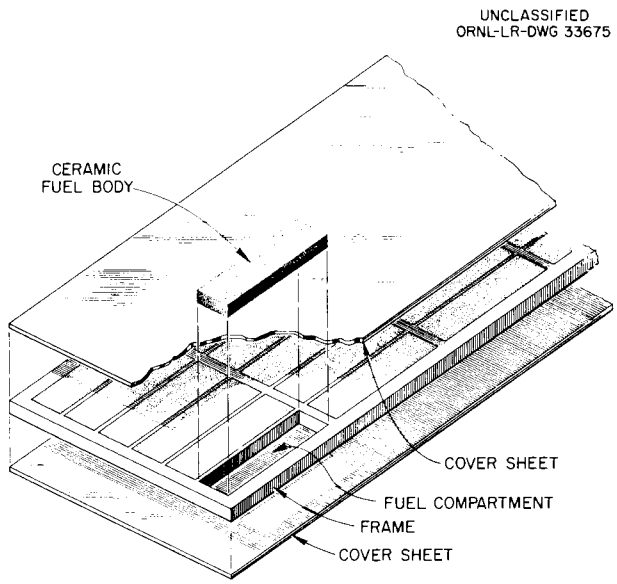

Fig. 4.7. Diagram of Compartmented Fuel Plate.

Two methods of fabricating the grid structure for these plates have been considered. One method involves the use of interlocking notched strips, and the other involves use of bent and spot-welded strips. The interlocking notched-strip design is shown in Fig. 4.8 and the bent-strip concept is illustrated in Fig. 4.9. Emphasis has been placed on the bent-strip grid because the manufacturing methods involved appear to be more economical. The strips required for the grid can be readily slit from sheet stock. Strips slit from 0.015-in.-thick, annealed, type 304 stainless steel to a nominal width of 0.194 in. actually varied by only ±0.001 in. from the nominal dimension.

[2]W. C. Thurber, Some Design Considerations in Compartmental Plate-Type Fuel Elements Containing UO_2, ORNL CF-58-7-105 (July 28, 1958).

UNCLASSIFIED
Y 27069

Fig. 4.8. Components Required for Compartmented Fuel Plate Assembled by Using Interlocking Notched-Strip Method.

Two techniques have also been considered for effecting the bond between the frame-grid structure and the cover sheets, namely, brazing and resistance welding. With the brazing technique, the cover sheets and frame-grid structure are plated with about 1 mil of electroless nickel. The frame, cover plates, and grid are then clamped between platens and brazed for 1/2 hr in hydrogen at 1850°F. The first plate manufactured by brazing utilized the interlocking notched strips for the grid. Each compartment in the plate was helium leak tested to determine whether or not it was hermetically sealed from all adjoining compartments. Of the 75 compartments in the plate, ten exhibited intercompartmental leakage. Subsequent plates have employed the bent-strip grid. With this type of structure, minimization of intercompartmental leakage has been considerably more difficult to achieve. All four of the plates made to date by this method have exhibited appreciably more leakage than the plate with the interlocking notched-strip grid. Consequently, a new welding jig has been designed to provide better alignment of the strips during spot welding. With this fixture, it is hoped that the number of interconnected compartments can be reduced significantly. An example of a sound bond between the grid and cover plate obtained by electroless nickel brazing is shown in Fig. 4.10.

Resistance-welding studies have indicated that this method of bonding cover sheets and frames is not acceptable for the particular geometry under investigation. With the relatively thin cover sheets (0.015 in.) and the relatively thick frame-grid structures (0.192 in.), it is impossible to generate enough heat at the interface of the cover sheet and the frame to effect bonding without overheating the outer surface of the cover where it contacts the electrodes. Attempts to place barrier sheets between the covers and electrodes did not yield satisfactory bonds. Although this bonding procedure was not successful with this particular geometry, it is probable that resistance welding can be used when the ratio of cover-plate thickness to total plate thickness is increased.

A limited amount of effort has been devoted to the manufacture of UO_2 fuel bodies for this type of element. Typical samples are illustrated

in Fig. 4.11. The length variation of these specimens was ±0.002 in. from the average and the width variation was ±0.001 in. from the average. Variations in thickness were appreciably greater, being on the order of ±0.005 in. from the average. Some taper was also noted in the thickness direction.

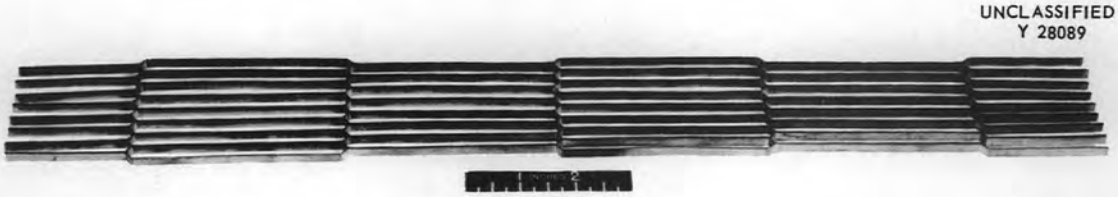

Fig. 4.9. Spot-Welded, Bent-Strip Grid for Compartmented Fuel Plate.

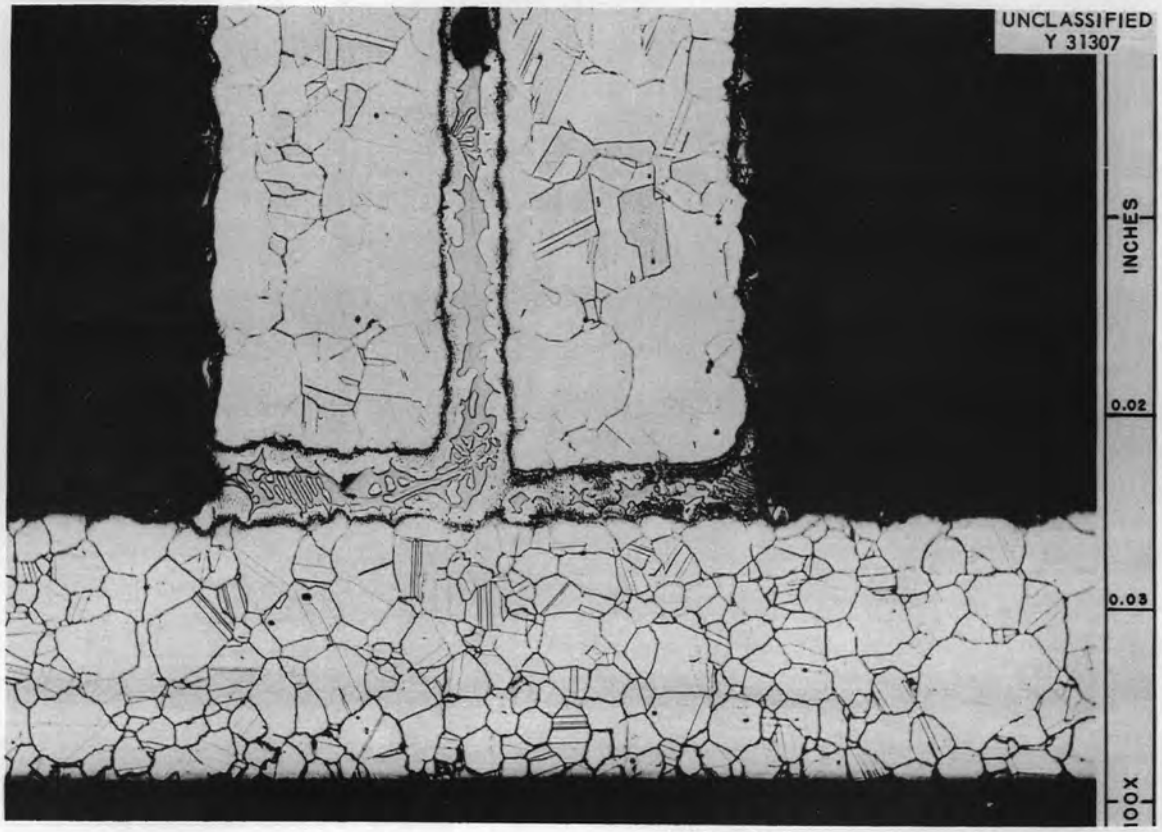

Fig. 4.10. Transverse Section Taken from Compartmented Fuel Plate No. 4 Illustrating Sound Bond Between Two-Ply Rib of Bent-Strip Grid and Cover Plate. Grid and cover are type 304 stainless steel and braze is electroless nickel. Etchant: 5% CrO_3, electrolytic (6 v, 4 sec).

UNCLASSIFIED
Y 30985

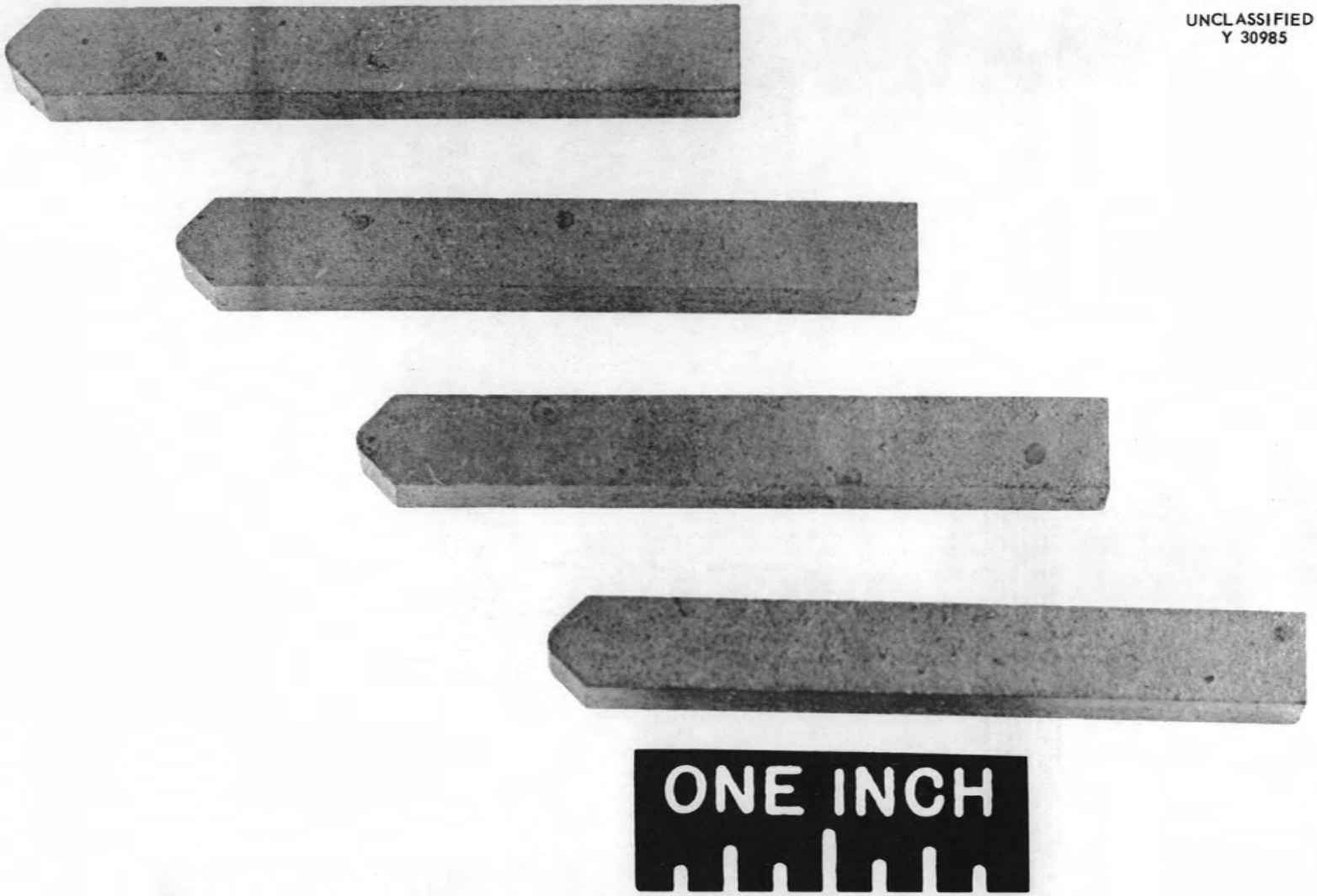

Fig. 4.11. Ceramic Fuel Bodies for Compartmented Fuel Plate.

Metal Heat Transfer Bonds

The replacement of helium by a low-melting metal in the annulus between fuel and cladding in elements of the type specified in Cores I and II of the N.S. Savannah reactor offers the possibility of minimizing peak fuel centerline temperatures significantly. Compatibility studies for 500 hr at 650 and 750°F on type 304 stainless steel-clad UO_2 fueled capsules with lead, bismuth, lead-bismuth eutectic, and Pb–0.7 wt % Li have indicated no deleterious effects with any of these bond metals in static tests. Lead was therefore selected for subsequent studies.

Tests were conducted to determine what effect a small amount of molten lead in the annulus between pellet and cladding would have on the integrity of a type 304 stainless steel fuel tube. Two 0.500-in-OD type 304 stainless steel tubes were filled with Lavite pellets (to simulate UO_2) and the annuli between the pellets and the tubes were completely filled with lead. The radial gap in one of the tubes was 0.015 in. and in the other tube it was 0.009 in. After filling, a 2-in. section in the center of each tube was inductively heated to 800°F and held for 15 min. Subsequent examination of the tubes showed that the expansion of the small area of liquid metal in the otherwise solid-lead annulus produced no dimensional changes. In addition, temperature cycling of one of the tubes 15 times between 400 and 800°F using the same induction-heating technique caused no dimensional changes. Radiographs of the tubes, however, showed discontinuities in the lead annuli, as shown in Fig. 4.12. Metallographic examination showed that although no lead had penetrated into the Lavite, definite void areas existed in the lead annulus in the heat-affected zones. Sections from the heat-affected area and from a sound, unaffected area are shown in Figs. 4.13 and 4.14.

The possibility of lead drainage from overheated, defective tubes was evaluated by autoclaving lead-filled capsules containing intentional defects at various temperatures. Results of these tests are presented in Table 4.6.

UNCLASSIFIED
Y 28087

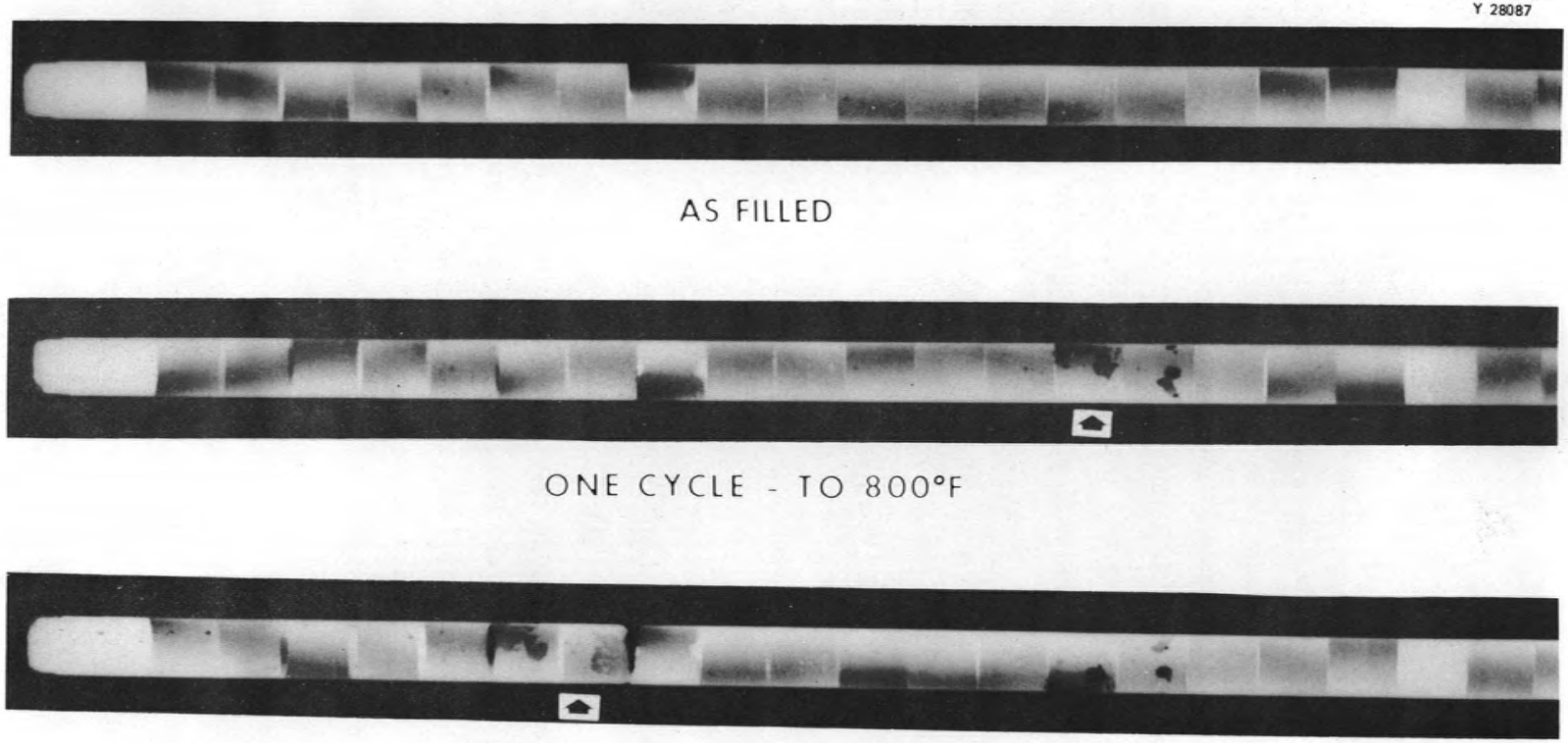

Fig. 4.12. Radiographs of Lead-Bonded Tubes.

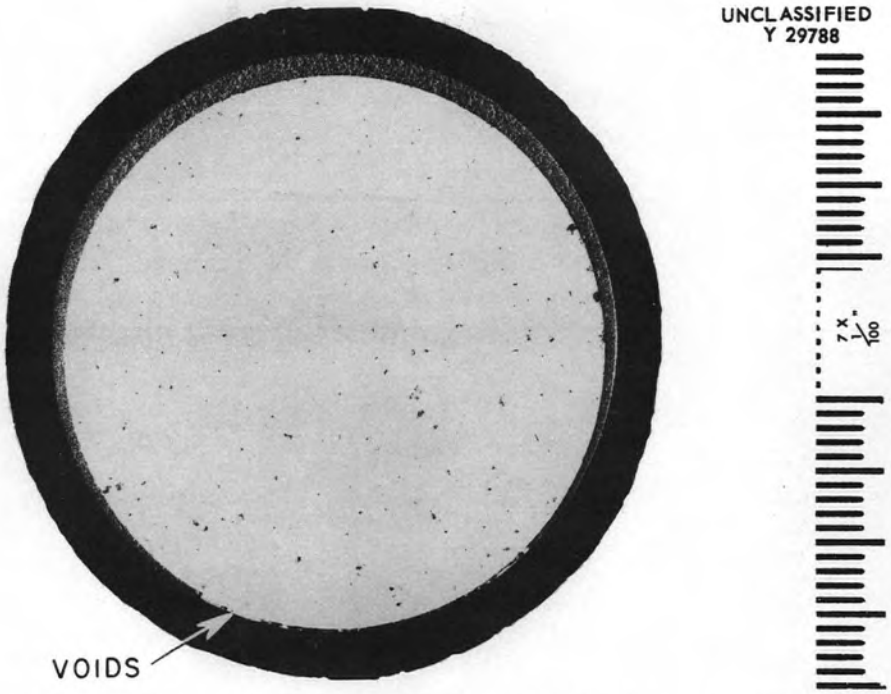

Fig. 4.13. Cross Section of Lead-Bonded Type 304 Stainless Steel Tube Containing Lavite Pellets. Section taken through area cycled 15 times between 400 and 800°F. Note discontinuities in lead annulus and absence of lead in Lavite. As-polished. Oblique illumination. 7X.

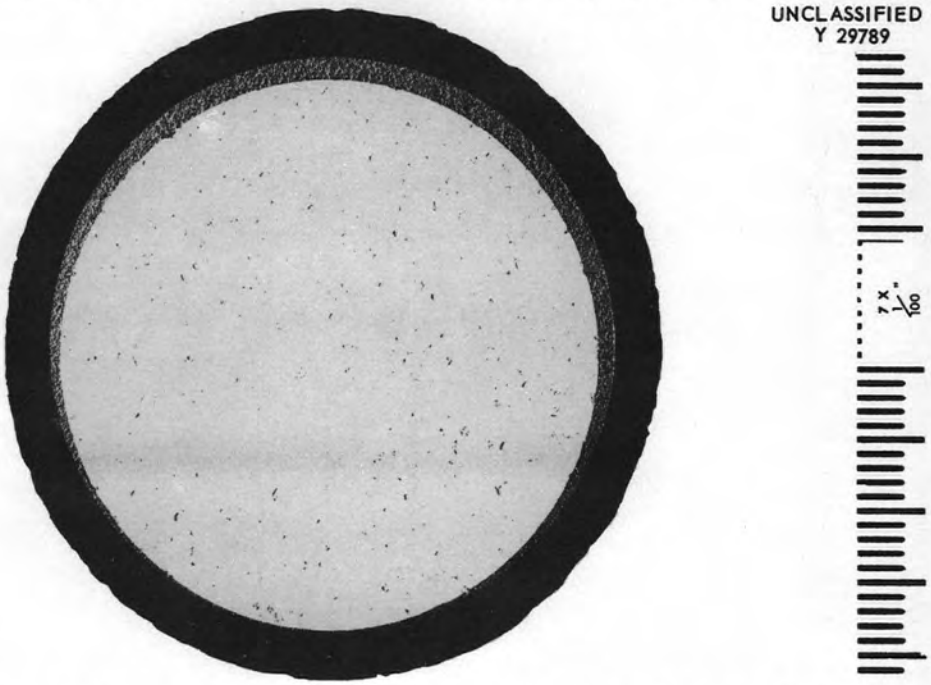

Fig. 4.14. Cross Section Through Unaffected Area of Tube Shown in Fig. 4.13. Note continuous annulus of lead. As-polished. Oblique illumination. 7X.

Table 4.6. Results of Tests of Lead Drainage From Annuli of Overheated Defective Capsules

Capsule No.	Temperature (°F)	Size of Defect (in.)	Duration of Heating (hr)	Drainage	Weight Change of Capsule (%)
1	650	0.015	400	No	+0.43
2	650	0.050	400	No	-0.044
3	700	0.050	24	Yes	
4	675	0.050	100 400	No Yes	+0.024
5	671–698	0.050	24	Yes	
6	599–617 636–644	0.050 0.050	24 24	No No	+0.70 +0.069

After 400 hr of heating, the defect holes in capsules 1 and 2 were filled with a reddish-orange crystalline deposit which was probably a lead oxide. Although capsule 4 did not show evidence of lead drainage during the first 100 hr of heating at 675°F, drainage occurred between the 100-hr and 400-hr examinations. It is thought that drainage was brought about by an upward temperature fluctuation in the autoclave furnace. To determine whether or not temperature fluctuations were the cause of drainage, a recorder was used to continuously monitor the furnace temperature during runs 5 and 6. Although the controller setting was nominally the same in both runs, 675°F, wide variations in temperature occurred. In the second part of run 6, the controller-temperature setting was reduced, but the resulting furnace temperature was higher. It may be concluded from the results shown in Table 4.6 that the possibility of lead drainage from tubing defects becomes a problem only at operating temperatures above 650°F.

In a preliminary effort to develop suitable techniques for inspecting lead-bonded fuel tubes, a purposely defective lead bond was made between Lavite pellets and a type 304 stainless steel fuel tube. The tube was inspected ultrasonically and radiographically. As shown in Fig. 4.15, good correlation was obtained between ultrasonically detected voids, indicated by lines and cross hatching on the tube, and radiographically indicated voids, shown as dark areas in the pellet column on the radiograph. Ultrasonic inspection and subsequent metallographic examination of a similarly bonded tube containing UO_2 pellets did not, however, result in such good correlation. In several areas, poor bonding was indicated by the ultrasonic inspection where a thin but continuous bond was actually present. In other areas, a sound bond was indicated where an equally thin lead bond existed. Areas of good and poor bond indications are illustrated in Figs. 4.16 and 4.17. Additional work is required to define the limits of this inspection technique.

In order to establish the feasibility of using lead-bonded fuel rods in braze-assembled fuel elements, a lead-bonded, Lavite-pellet-filled tube was held at 1900°F in hydrogen for 4 hr and then examined. Although no dimensional changes were noted after this treatment, a radiograph of the tube showed that the bond continuity was seriously impaired. The lead, which had originally been a continuous film between the pellets and the tube, appeared as fine droplets on the tube wall, and the Lavite pellets, which were originally white, were gray, indicating that they probably had absorbed some lead. This rather complete deterioration of the lead thermal bond indicates that lead bonding may be used in mechanically joined element or in brazed elements only if the bonding metal is injected after completion of brazing.

Several methods of filling the annulus between the fuel and cladding with lead have been briefly investigated. The intent of this study was to investigate the general feasibility of various filling methods rather than to develop any one particular technique. The three techniques studied were: (1) pouring molten lead into a heated, loaded tube, (2) immersing a loaded tube in a bath of molten lead, and (3) filling an

UNCLASSIFIED
Y 28625

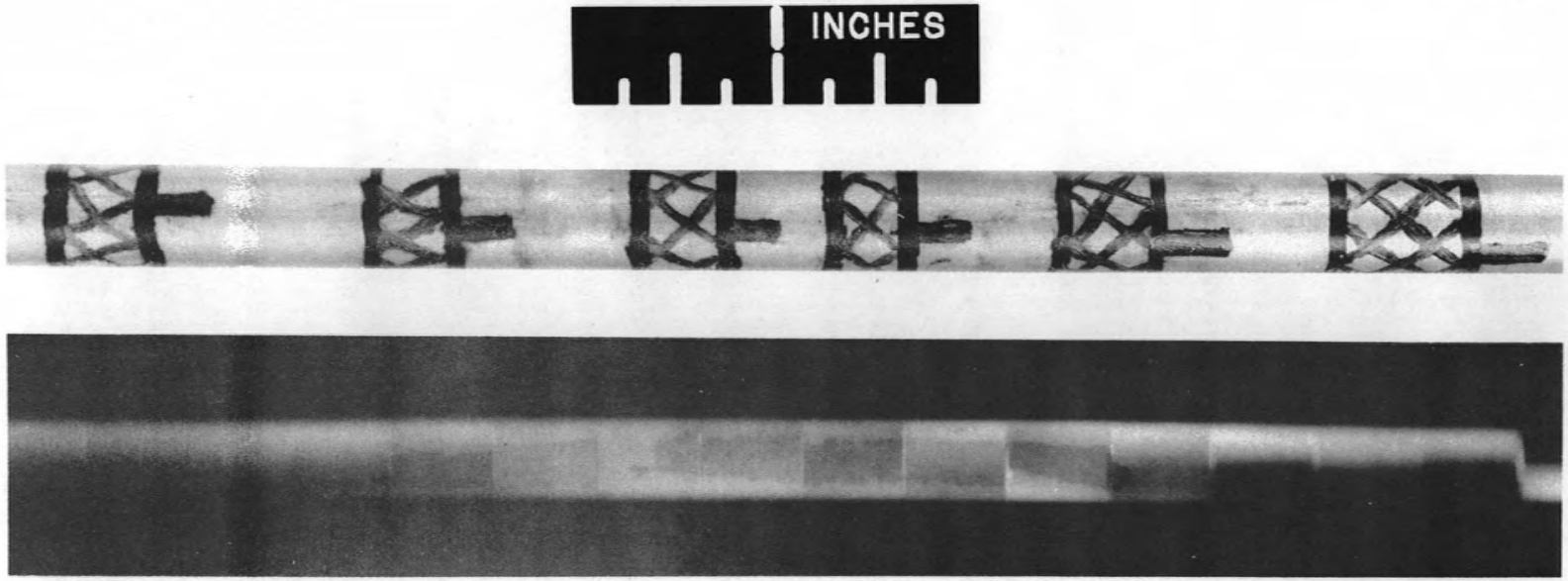

Fig. 4.15. Correlation Between Ultrasonically Detected Voids (Top) and Radiographically Indicated Voids (Bottom) in Lead-Bonded Fuel Tube.

Fig. 4.16. Section of Lead-Bonded UO_2-Filled Type 304 Stainless Steel Tube Showing Lead Annulus. Ultrasonic inspection indicated good bonding. The extremely thin section of lead indicates the degree of wettability of UO_2 and stainless steel by lead. As-polished. Oblique illumination. 7X.

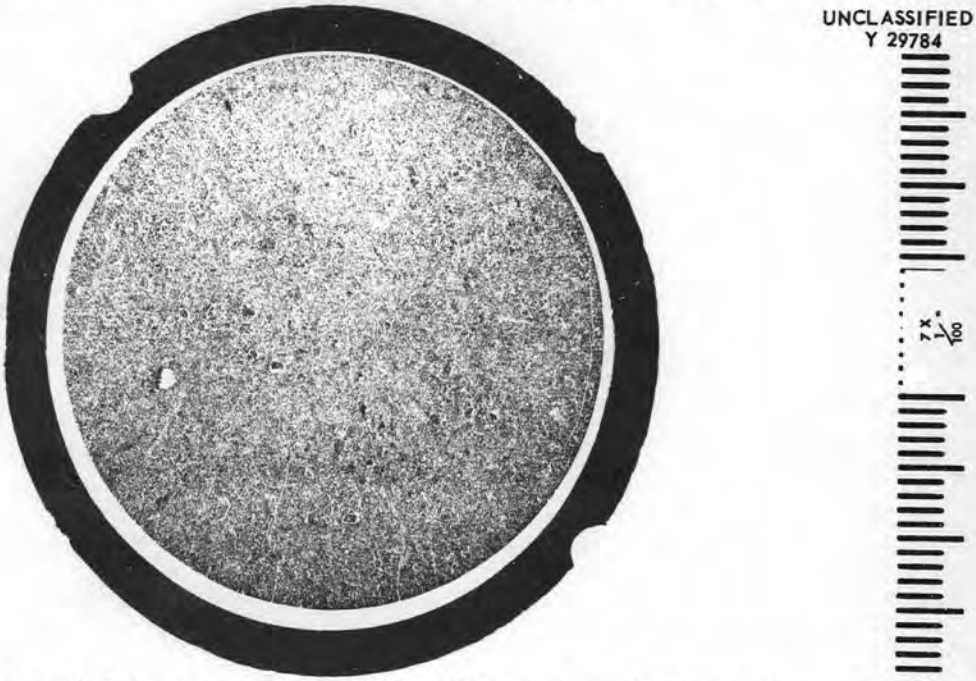

Fig. 4.17. Lead-Bonded UO_2-Filled Type 304 Stainless Steel Tube Showing Lead Annulus. Ultrasonic inspection indicated only partial bonding in the area shown. As-polished. Oblique illumination. 7X.

empty tube with lead and then inserting heated pellets. After filling, directional solidification of the molten metal from the bottom was promoted with a water quench to minimize void formation due to shrinkage cavities. To date, only one of the three techniques investigated, immersing loaded tubes in a molten-lead bath, has produced lead bonds of consistent quality. It was impossible to produce a good bond at the bottom of a column by pouring molten lead into the loaded tubes because of inefficient release of entrapped air. An incompletely loaded tube resulted when heated pellets were inserted into a lead-filled tube because the pellets had not been heated to a sufficiently high temperature. To achieve the higher pellet temperatures required in methods 1 and 3 without serious pellet oxidation it will be necessary to fill the tubes either under an inert atmosphere or in a vacuum.

Irradiation Studies

A tentative program has been devised for the irradiation studies to be carried out in the pressurized-water in-pile test loop described in Chap. 3. As presently conceived, the program involves irradiation of both swaged UO_2-bearing fuel rods and rods containing cold-pressed and sintered UO_2 pellets. In the tests on swaged rods, an attempt will be made to determine the effects of various parameters, such as UO_2 particle size, fuel temperature, swaging temperature, and exposure time, on general performance and fission-gas release. Irradiation of rods containing cold-pressed and sintered pellets will produce data needed to correlate conductivity and width of the gas gap with central melting in order to obtain a more valid heat-transfer model for this type of fuel element.

Work is in progress to devise means of fabricating test specimens for the loop. This involves both fabrication of individual rods by swaging techniques and assembly of these rods into three-rod clusters. It appears that the three-rod cluster can be assembled by brazing with electroless-nickel-plated ferrules. A test bundle assembled in this manner is shown in Fig. 4.18.

UNCLASSIFIED
Y 32374

Fig. 4.18. Fuel Element Fabricated by Brazing with Electroless Nickel-Plated Ferrules.

A cooperative program has been initiated with Atomic Energy of Canada, Limited, in which psuedo-diffusion coefficients,[3] D', will be measured at the Chalk River Laboratory on various UO_2 fuels of interest to ORNL programs. Included in this work will be measurements of D' values for (1) pressurized-water-loop fuel pellets produced by Union Carbide Nuclear Company (Y-12 Plant), (2) N.S. Savannah Core-I pellets produced from virgin UO_2 by Babcock & Wilcox Company, (3) N.S. Savannah Core-I pellets produced from recycled UO_2 by Babcock & Wilcox Company, (4) N.S. Savannah Core-II pellets produced from virgin UO_2 by General Electric Company. Attempts will be made to correlate the measured D' values with manufacturing history, open porosity, grain size, and density. Pellets fabricated at the Y-12 Plant have been shipped to Chalk River.

Analysis of Primary System Components for Cobalt and Other Trace Elements

Samples of 15 components from the N.S. Savannah primary system have been analyzed for cobalt, tantalum, silver, antimony, and zinc. These elements were selected as potential contributors to long-lived activity in the pressurized-water plant. Results of these analyses, presented in Table 4.7 indicate, in general, that the quantities of all the elements assayed, except cobalt, fall below the lower limits of detection of the selected analytical methods. The cobalt content was less than 0.1% in all the components sampled except the outer thermal shield. Two of the heats used in that structure had cobalt contents of 0.29 and 0.84%.

Evaluation of Brittle Fracture Characteristics of the N.S. Savannah Pressure Vessel

Samples of the type SA-212, grade B, carbon-silicon steel used in both the upper and lower closure heads of the N.S. Savannah pressure vessel were obtained from the Babcock & Wilcox Company for testing. Unfortunately, no material representative of the cylindrical shell of

[3] A. H. Booth, A Method for Calculating Fission-Gas Diffusion from UO_2 Fuel, CRDC-721 (Sept. 1957).

Table 4.7. Analysis of N.S. Savannah Primary System Components Long-Lived Gamma-Emitting Elements

	Component Identification	Element (wt %)				
		Co	Ta	Ag	Sb	Zn
1.	MK-300, heat-22453-3T, upper plate	0.098	<0.003	<0.0001	<0.0005	<0.0005
2.	MK-509, heat-24948, flow tube	0.071	<0.003	<0.0001	<0.0005	<0.0005
3.	MK-509, heat 24841, flow tube	0.062	<0.003	<0.0001	<0.0005	<0.0005
4.	Heat 22141-2E, outer thermal shield	0.73 0.82 0.97[a]	<0.003 <0.003	<0.0001 <0.0001	<0.0005 <0.0005	<0.0005 <0.0005
5.	Heat NP-960, primary gate valves	0.058	<0.003	<0.0001	<0.0005	<0.0005
6.	MK-301, heat 22458-IT, lower plate	0.082	<0.003	<0.0001	<0.0005	<0.0005
7.	MK-304, heat 24839, tube half	0.066	<0.003	<0.0001	<0.0005	<0.0005
8.	MK-302, heat 24770, flow tube	0.074	<0.003	<0.0001	<0.0005	<0.0005
9.	670-0011-60, heat A-3415, primary piping	0.038	<0.003	<0.0001	<0.0005	<0.0005
10.	670-0011-45, heat 335836-5, primary piping	0.074	<0.003	<0.0001	0.001	<0.0005
11.	670-0006-51, heat X-22078-2T, outer thermal shield	0.091	<0.003	<0.0001	<0.0005	<0.0005
12.	670-0006-51, heat X-22160-ID, outer thermal shield	0.29	<0.003	<0.0001	<0.0005	<0.0005
13.	670-0007-53, heat 14620-X, heat exchanger tube	0.069	<0.003	<0.0001	<0.0008	<0.0005
14.	670-0007-53, heat 24046-X, heat exchanger tube	0.045	<0.003	<0.0001	<0.0005	<0.0005
15.	Cladding from inner surface of upper closure head of pressure vessel	0.042	<0.003	<0.0001	<0.0005	<0.0005

[a]This result obtained at ORNL; all other analyses performed by Lucius Pitkin, Inc., New York.

the vessel was available for study. Scrap material from the upper closure head had received essentially the same heat treatments as the head itself. Scrap from the lower closure head was not representative of the final component and consequently was tested both in the as-received condition and after normalization and stress relief.

The steel was evaluated by determining the nil-ductility transition (NDT) temperature as defined by the Naval Research Laboratory drop-weight test and correlating these results with the Charpy-V notch impact energy at the same temperature. It was determined that the NDT temperature was 20°F or less for all materials tested in the normalized and stress-relieved condition. This temperature was correlated with a Charpy-V notch impact energy of 20 ft-lb. Steel in the as-received condition had an appreciably higher NDT temperature of 50°F, emphasizing the importance of proper heat treatment in reducing the temperature at which brittle fracture can occur.[4]

Electroless-Nickel Brazing Studies

The feasibility of using electroless nickel, a chemically deposited plate containing about 10 wt % phosphorus in nickel, as the brazing alloy for the assembly of the N.S. Savannah fuel bundles was investigated.[5] By plating this alloy on the spacer ferrules of the fuel bundle, the problem of preplacing a powdered brazing alloy in a multitude of joints could be eliminated.

It was concluded that this material was generally suitable for the proposed application, since the electroless nickel readily wetted the stainless steel and produced adequate fillets. The electroless nickel did not undercut and alloy significantly with the type 304 stainless

---

[4]W. C. Thurber and J. T. Lamartine, Determination of the Nil-Ductility Transition Temperature for A212B Steel Used in N.S. Savannah Pressure Vessel, ORNL CF-59-7-143 (July 23, 1959).

[5]J. T. Lamartine and W. C. Thurber, Status Report – Application of Electroless-Nickel Brazing to Tubular Fuel Elements for the N.S. Savannah, ORNL CF-59-6-55 (June 2, 1959).

steel components of the fuel bundle, and thus the integrity of the fuel tubes was in no way jeopardized.

Microstructurally the fillets were characterized by a ductile solid solution region 15 to 25 mils wide at the center of the fillet where the joint spacing was smallest. Adjacent to this was a brittle area containing appreciable quantities of the intermetallic compound Ni_3P. Although cracks were often noted in this outer region, they did not appear to propagate through the solid solution zone.

Relatively rigorous thermal cycling (25 cycles) of an 8-in.-long, 16-tube bundle brazed with electroless nickel did not appear to impair the quality of the joints. For cycling, the bundle was immersed in a lead bath at 770°F, removed, and quenched in an air blast to 220°F. Metallographic examination of brazed joints in the bundle after the 25 cycles revealed no crack propagation through the fillets. Joint-strength test specimens subjected to the same treatment failed at loads identical to those at which uncycled control specimens failed.

The mechanical strength of joints brazed with electroless nickel was essentially the same as that of similar joints prepared with the use of Nicrobraz No. 50 as the bonding agent. Shear strengths determined by the Miller-Peaslee test were 23,800 psi and 29,100 psi for electroless-nickel and Nicrobraz No. 50 brazed joints, respectively. The quality and character of electroless-nickel brazed joints appeared to be insensitive to brazing conditions over the temperature range 1750 to 1900°C with brazing times of 15 to 180 min.

A sample of type 304 stainless steel sheet with a coating of electroless nickel brazed on one surface and a sample of fuel tube-to-ferrule joint made with electroless nickel were corrosion tested for 1300 hr in oxygenated, deionized water at 525°F. The corrosion resistance of the samples was excellent, with the over-all corrosion rate being 0.1 mil/yr or less. No localized attack was noted. Electroless nickel is now being employed by the Babcock & Wilcox Company in the fabrication of Core I fuel bundles for the N.S. Savannah.

Pyrometer Wire Studies

A major problem in interpreting results of irradiation experiments on UO_2-bearing fuel rods is to arrive at a valid estimate of the fuel temperature. In order to minimize the uncertainties associated with this temperature estimate, it was proposed to insert small-diameter wires of various known melting points at selected radial locations in the UO_2 pellets and to determine by postirradiation metallography whether or not melting of a particular wire at a given location had occurred. In furtherance of this concept, compatibility studies of Cu, Au, Ni, Fe, Pt, V, and Nb with UO_2 were conducted at various temperatures.[6]

On the basis of the experiments performed it was concluded that the temperature-monitoring technique was not generally practicable with the materials studied. Copper and gold were found to be compatible with UO_2 at 1300 and 1400°C, respectively. At higher temperature these wires react with UO_2. Gold, however, can undergo appreciable transmutation to mercury, which would confuse metallographic interpretation of postirradiation structures. Nickel reacts with UO_2 at temperatures as low as 1300°C. The reaction is characterized by eutectic formation. The behavior of iron is similar to that of nickel with reactions occurring at 1300 to 1500°C. Platinum reacts with UO_2 at temperatures as low as 1300°C (that is, at 470°C below its melting point). Reaction between vanadium and UO_2 occurs in the temperature range 1660 to 1900°C, with the formation of an extremely hard substance of unknown composition. In short-time experiments niobium is compatible with UO_2 to 1800°C. Because of equipment limitations no information was obtained on the stability of this system at higher temperatures. However, recent information[7] indicates that UO_2 will react rapidly with niobium at 2065°C.[8]

---

[6]W. C. Thurber and R. E. Meadows, Feasibility Study – Use of Small Diameter Wires in UO_2 Pellets for In-Pile Temperature Monitoring, ORNL CF-59-10-7 (to be issued).

[7]Met. Ann. Prog. Rep. Sept. 1, 1959, ORNL-2839, p 294.

[8]This is an uncorrected optical pyrometer temperature. When an emmissivity correction is applied the true temperature is somewhat higher.

5. PHYSICS

Techniques for analyzing the physics of reactor cores of the type used for the N.S. Savannah are being studied. In these studies, mathematical models are being developed which are consistent with existing critical experiment data on the Savannah core. The techniques so developed will be useful in evaluating changes from the present design, as well as in guiding the direction of future core design work.

The central problem of reactor analysis is the determination of reaction rates in the various reactor materials. One requirement for the successful solution to this problem is an adequate determination of the flux distribution within the reactor. This is especially important in Savannah-type cores because of the many material inhomogeneities present in the design. The heterogeneous nature of this core is illustrated by Figs. 5.1, 5.2, and 5.3. The arrangement of the 32 fuel element cans and the 21 control rod cruciforms is shown in Fig. 5.1; Fig. 5.2 gives the details of a fuel element can used in the Marty VI critical experiment;[1] and Fig. 5.3 gives the details of a critical experiment fuel pin.

Since diffusion theory is inadequate for determining the flux distribution within a fuel pin cell, the S-4 approximation[2] to the neutron angular transport equation was employed for studying the flux distribution. Some results obtained from the S-4 calculations of flux distribution within a fuel pin unit cell are shown in Fig. 5.4. The fluxes plotted in Fig. 5.4 have been arbitrarily normalized to a value of 1 at the outer boundary of the fuel pin cell. The curves demonstrate that the usual assumption of a "flat" fast-flux spatial distribution is not very good for all epithermal groups in Savannah-type fuel pin cells.

---

[1]R. M. Ball *et al.*, Critical Experiments for the N.S. Savannah Core, BAW-1131 (Dec. 10, 1958).

[2]B. G. Carlson and G. P. Bell, Solution of the Transport Equation by the S_n Method, Geneva Conference Paper 2386 (1958).

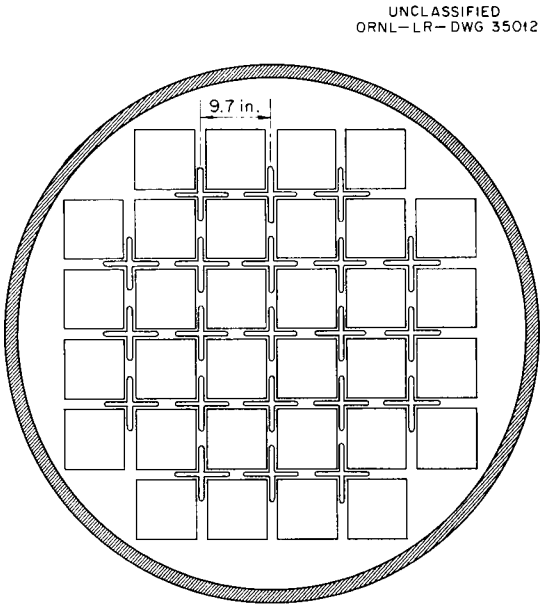

Fig. 5.1. Core Configuration of N.S. Savannah Reactor.

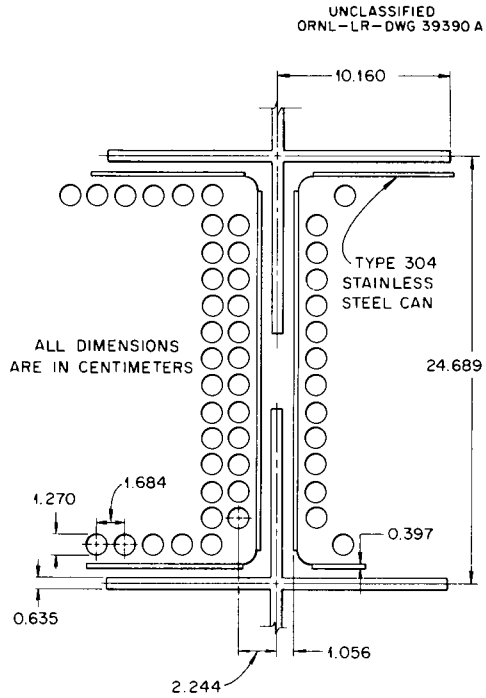

Fig. 5.2. Portion of Marty VI Critical Experiment Core.

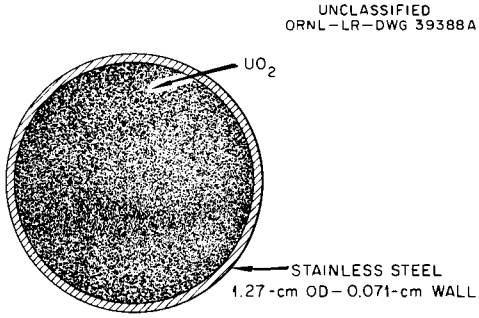

Fig. 5.3. Marty VI Critical Experiment Fuel Pin.

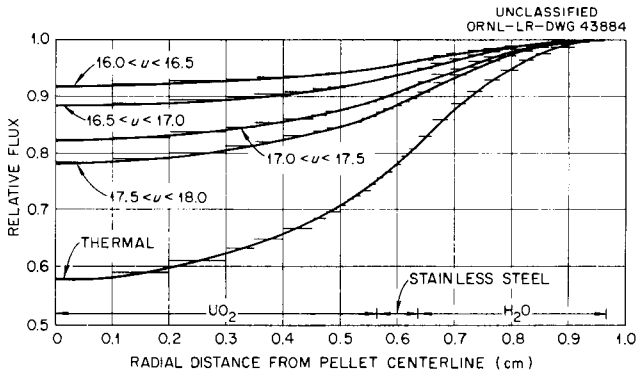

Fig. 5.4. Marty VI Fuel Pin Cell Flux Profiles (SNG-S4 Results).

Even in the lethargy interval $16.0 < u < 16.5$ (0.68 ev $< E < 1.13$ ev) the flux in the UO_2 is some 6% less than the flux in the surrounding water.

The results presented in Fig. 5.4 allow the homogeneization of the fuel pin region within a fuel element can. Flux distributions across a homogeneous fuel pin region and into the water channel between fuel element cans are presented in Fig. 5.5. The severe peaking of the thermal flux in the water channel has necessitated the use of Zircaloy followers on the ends of the control rods in the final design of Core I. These Zircaloy followers displace water and thereby reduce the peaking between fuel element cans.

The results given in Fig. 5.5 were obtained using one-dimensional transport theory. An investigation of the importance of possible two-dimensional effects occurring at the corners of each fuel element can was made with the use of a two-dimensional diffusion theory machine code[3] for the IBM 704. The two-dimensional representation used for Marty II[4] is shown in Fig. 5.6 Notice that the missing corner pin is accounted for by extending the water region into the corner of the fuel pin region. The thermal utilizations predicted by one-dimensional diffusion theory, one-dimensional transport theory, and two-dimensional diffusion theory are compared in Table 5.1.

Comparison of the one-dimensional diffusion theory and the one-dimensional transport theory results indicates that diffusion theory is quite adequate for a Savannah-type fuel element can cell. The two-dimensional model gives a small correction to the one-dimensional thermal utilization result. However, the two-dimensional results are much more significant when regarded from the flux peaking point of view, as may be seen by examination of Fig. 5.7, which presents flux profiles across a Marty II fuel element can. In Fig. 5.7, the pronounced thermal flux peaking in the corner of a fuel can is quite evident.

---

[3]G. G. Bilodeau et al., PDQ, An IBM-704 Code to Solve the Two-Dimensional Few-Group Neutron Diffusion Equation, WAPD-TM-70 (1957).

[4]Babcock & Wilcox Co., NMSR Proj. Quar. Tech. Rep., January – March 1958, BAW-1102, pp 51-54.

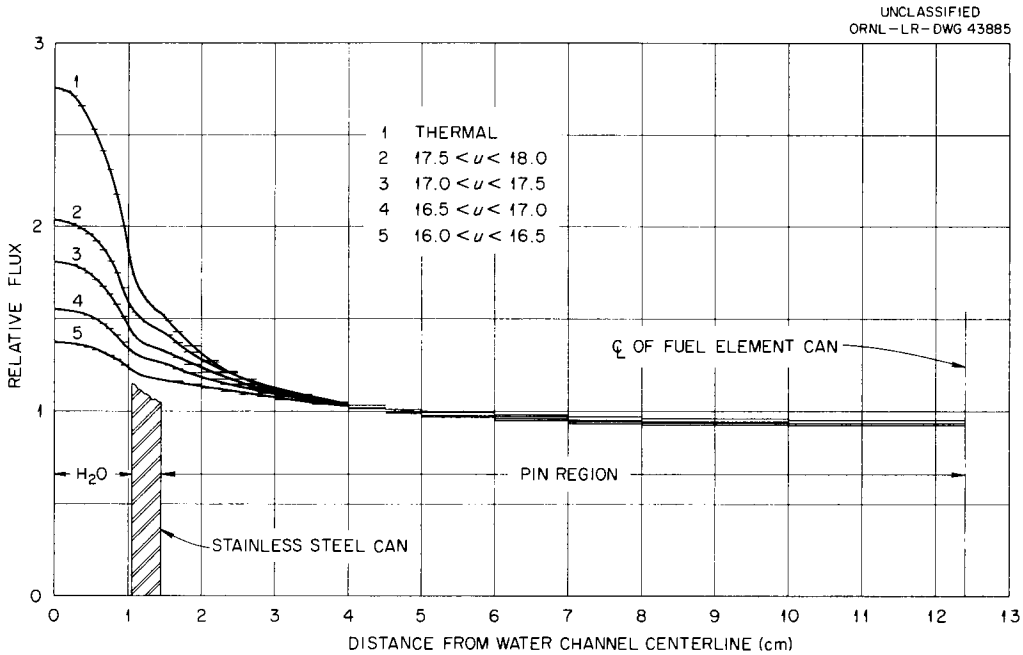

Fig. 5.5. Flux Profiles in Marty VI Fuel Element Can Cell (Φ = 1.0 in Pin Region).

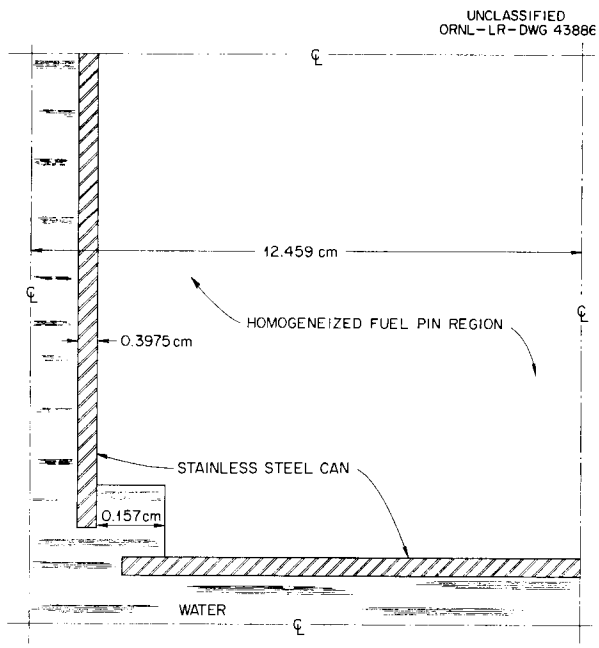

Fig. 5.6. One Quadrant of Marty II Fuel Element Can Cell.

Table 5.1. Effect of Analytical Model on Thermal Utilization Values for Marty II Can Cell

Analytical Model	Thermal Utilization
One-dimensional diffusion theory	0.638
One-dimensional transport theory	0.635
Two-dimensional diffusion theory	0.627

Also presented in Fig. 5.7 is the experimental thermal flux profile,[5] which may be seen to fall below the diffusion theory and transport theory predictions in the water channel region. The calculated flux profiles were obtained by assuming (1) that the epithermal flux (the source for thermal neutrons) is flat across a fuel element can and (2) that the neutron temperature characterizing the thermal neutron Maxwellian spectrum is the same in the water channel as it is in the homogeneized fuel pin region. Experimental epicadmium flux measurements[6] indicate that the epithermal flux in the water channel may be 10 to 20% less than in the fuel pin region.

The effect on the thermal flux distribution of various assumptions concerning the epithermal flux distribution are shown in Fig. 5.8. A 10% smaller fast flux in the water channel relative to that in the fuel pin region is seen to be sufficient to obtain agreement with the observed thermal flux profile. Taking the neutron temperature in the fuel pin region to be about 47°C above the neutron temperature in the water channel is also sufficient to obtain agreement with the measured flux profile. This neutron temperature difference is about the amount one would expect on the basis of the thermal spectrum hardening results

---

[5]Babcock & Wilcox Co., NMSR Proj. Quar. Tech. Rep., April – June 1958, BAW-1118, Fig. 13, together with the cadmium ratio results reported on p 31.

[6]Babcock & Wilcox Co., NMSR Proj. Quar. Tech. Rep., January – March 1959, BAW-1145, Figs. 26 and 30.

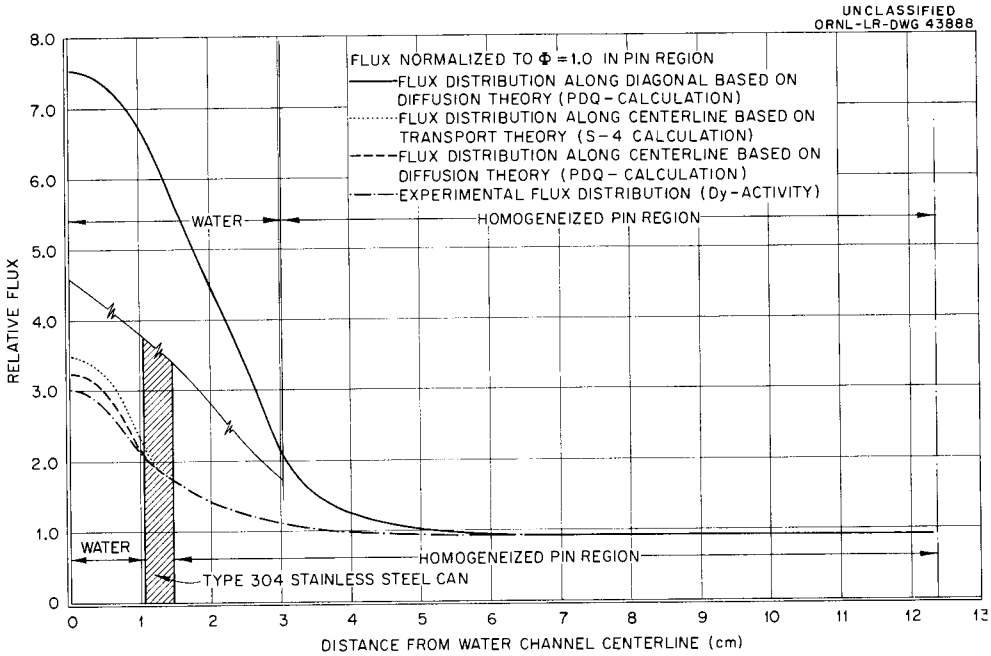

Fig. 5.7. Neutron Flux Distribution in Can Cell of Marty II.

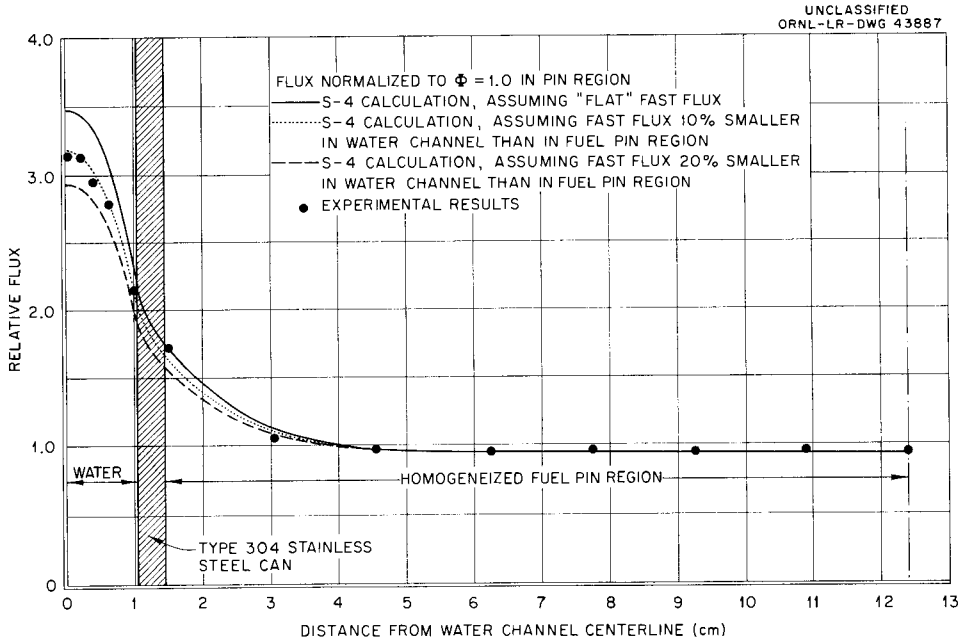

Fig. 5.8. Thermal Flux Profile Across Marty II Fuel Can.

of Brown and St. John[7] if it is assumed that no hardening occurs in the 3/4-in.-wide water channel. It is likely that the actual thermal flux profile depends on some combination of spectra hardening and epithermal flux variation, but the present data are incapable of unraveling the relative importance of these two effects.

The techniques described above for obtaining thermal flux distribution in a heterogeneous system have been applied to the Core I design. Details of a Core I fuel element are shown in Fig. 5.9, which is a cross section through a ferrule region of the core. The ferrules, which are 1-in.-long stainless steel tubes spaced every 8 1/8 in. along the axial direction, give rigidity to the fuel element bundle. For two-dimensional can cell calculations, the Core I fuel element was approximated by the geometry shown in Fig. 5.10. The thermal flux results for Core I are schematically illustrated in Fig. 5.11, which gives the average flux in each core region relative to a value of 1 for the average flux in the UO_2. The inhomogeneous nature of Core I from the thermal flux standpoint is quite evident in Fig. 5.11.

Thermal neutron reaction rates determine only part of the neutron balance. To complete the neutron balance epithermal reaction rates are also needed. The importance of epithermal neutrons for this reactor becomes evident when it is realized that greater than 25% of the fissions are epithermal fissions. Unfortunately, in addition to the well-known inadequacies of present-day hydrogen slowing-down theory, many of the important epithermal cross sections are not known to accuracies better than ±20%. As an example of the sensitivity of Savannah-type cores to epithermal cross sections, it is estimated that a 10% reduction of the U^{235} fission resonance integral (this amount is within present uncertainty) would increase the predicted Marty VI critical radius by about 8%.

Using nominal values for epithermal cross sections (including inelastic scattering) and the thermal homogeneization procedure outlined

---

[7]H. D. Brown and D. S. St. John, Neutron Energy Spectrum In D_2O, DP-33 (February 1954).

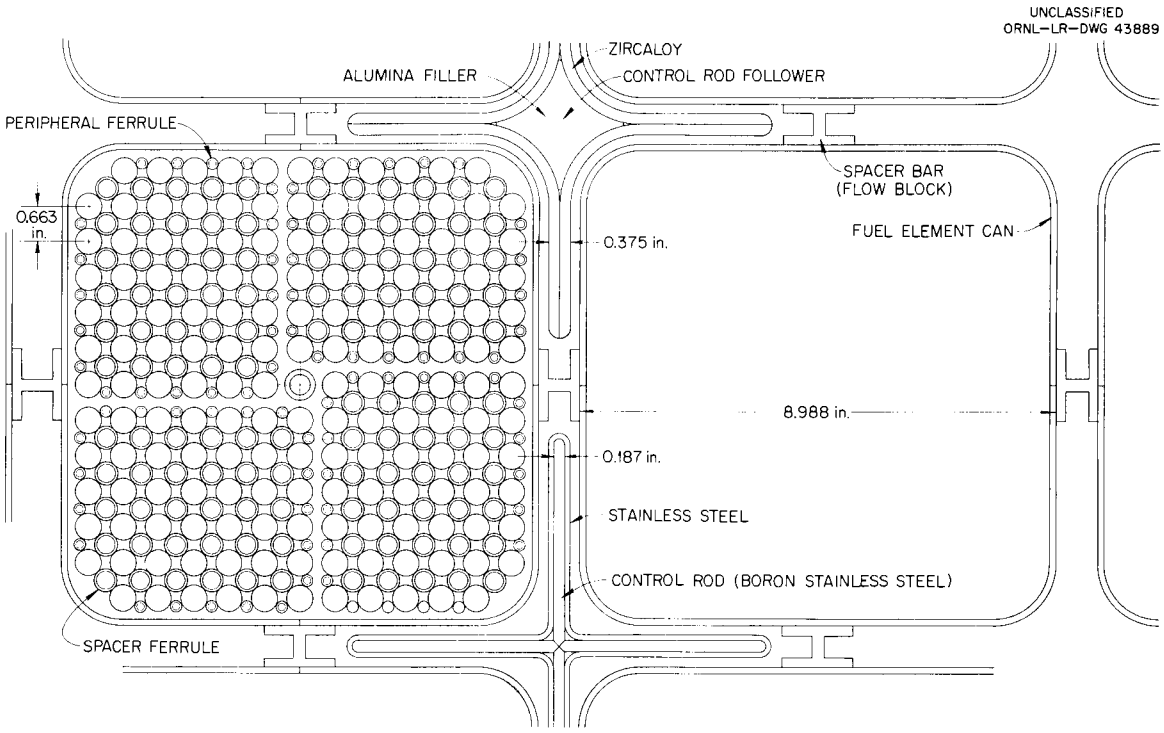

Fig. 5.9. Portion of Core I.

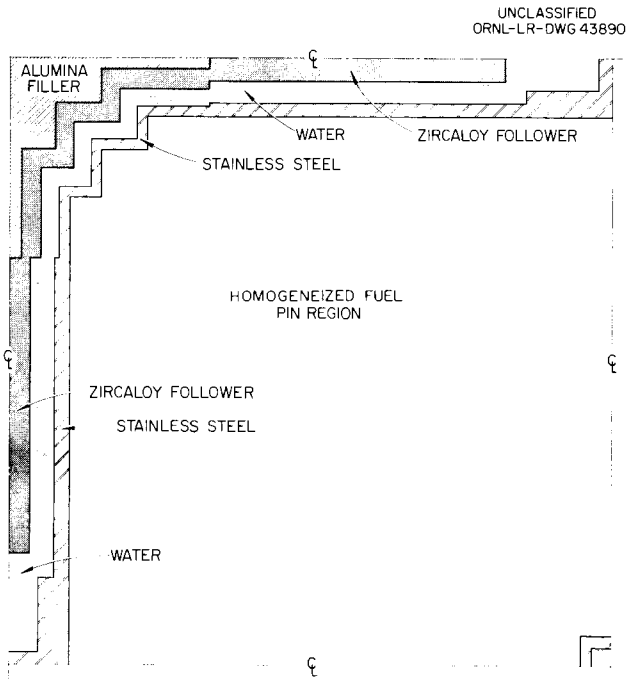

Fig. 5.10. One Quarter of Core I Can Cell.

above, the effect of replacing the stainless steel cans by Zircaloy cans has been evaluated for Core I. Preliminary results of this investigation are presented in Fig. 5.12. The calculated k_{eff} value for Core I may be compared with a value of $k_{eff} = 1.11 \pm 0.01$ obtained[8] by extrapolation from critical experiment data. The disagreement of the calculated value and the measured value for Core I should not invalidate the comparison between a stainless steel can core and a Zircaloy can core. The data of Fig. 5.12 indicate that a Zircaloy can core would contain the same cold reactivity as the present core with 3.1% enriched UO_2 rather than the present 4.2% enriched fuel.

---

[8]Babcock & Wilcox Co., Summary of N.S. Savannah Core Physics (March 18, 1959) transmitted in a letter, C. W. Hasek, Jr., to C. R. McFarland (March 24, 1959).

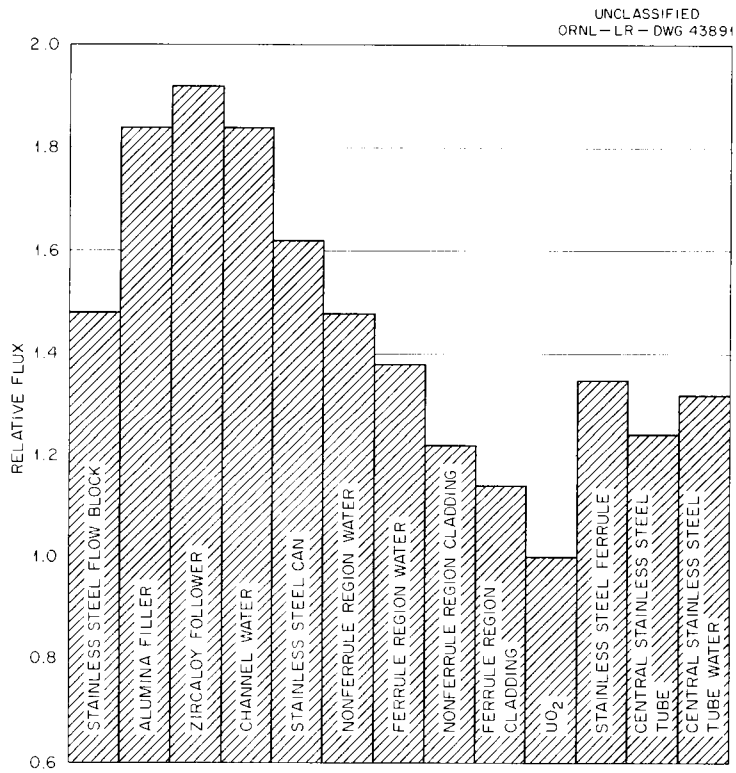

Fig. 5.11. Calculated Average Thermal Flux Values for Core I. Thermal flux in UO_2 normalized to 1.

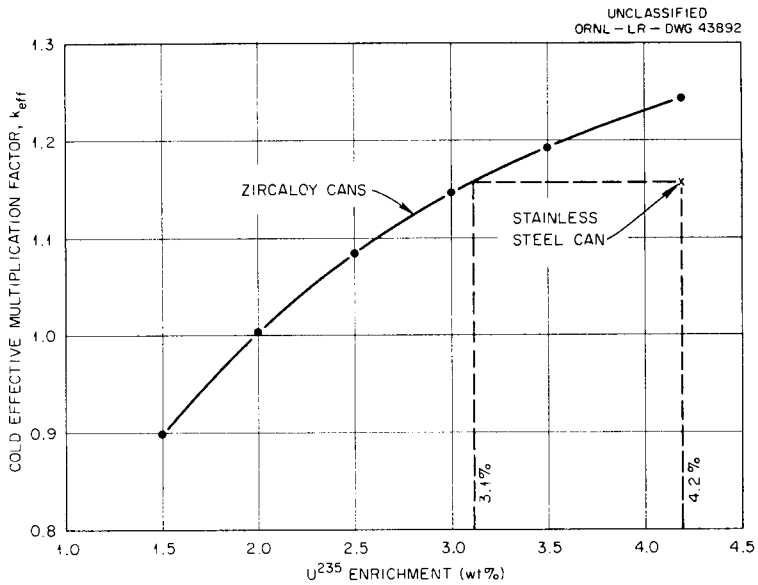

Fig. 5.12. Comparison of Stainless Steel and Zircaloy Cans in Core I.

ORNL-2865
Reactors—Power
TID-4500 (15th ed.)

INTERNAL DISTRIBUTION

1- T. D. Anderson
2- V. E. Anderson (K-25)
3- R. J. Beaver
4- D. S. Billington
5- R. E. Blanco
6- E. P. Blizard
7- A. L. Boch
8- C. J. Borkowski
9- G. E. Boyd
10- E. J. Breeding
11- R. B. Briggs
12- F. R. Bruce
13- T. J. Burnett
14- C. E. Center (K-25)
15- R. A. Charpie
16- T. E. Cole
17- J. A. Conlin
18- W. B. Cottrell
19- J. A. Cox
20- F. L. Culler
21- H. N. Culver
22- J. E. Cunningham
23- L. M. Doney
24- I. T. Dudley
25- J. C. Ebersole
26- L. B. Emlet (K-25)
27- E. P. Epler
28- W. K. Ergen
29- A. P. Fraas
30- J. H. Frye, Jr.
31- W. R. Grimes
32- E. E. Gross
33- E. Guth
34- J. C. Hart
35- V. O. Haynes
36- R. L. Heestand
37-38- M. R. Hill
39- R. R. Holcomb
40- A. Hollaender
41- A. S. Householder
42- W. H. Jordan
43- S. I. Kaplan
44. P. R. Kasten
45. C. P. Keim
46. M. T. Kelley
47. R. B. Korsmeyer
48. J. T. Lamartine
49. J. A. Lane
50. R. S. Livingston
51. H. G. MacPherson
52. W. D. Manly
53. E. R. Mann
54-56. H. C. McCurdy
57. A. J. Miller
58. E. C. Miller
59. K. Z. Morgan
60. J. P. Murray (Y-12)
61. F. H. Neill
62. M. L. Nelson
63. P. Patriarca
64. A. M. Perry
65. D. Phillips
66. M. E. Ramsey
67. P. M. Reyling
68. J. T. Roberts
69. J. E. Rowe (K-25)
70. A. F. Rupp
71. H. W. Savage
72. A. W. Savolainen
73. L. D. Schaffer
74. O. Sisman
75. E. D. Shipley
76. M. J. Skinner
77. G. M. Slaughter
78. A. H. Snell
79. P. E. Stein (Y-12)
80. J. A. Swartout
81. E. H. Taylor
82. W. C. Thurber
83. D. B. Trauger
84. A. M. Weinberg
85. G. C. Williams
86. C. E. Winters
87. M. L. Winton

88-91. ORNL – Y-12 Technical Library Document Reference Section
92-103. Laboratory Records Department
104. Laboratory Records, ORNL R.C.
105-107. Central Research Library

EXTERNAL DISTRIBUTION

108-117. Division of Reactor Development (Maritime Reactors), AEC, Washington (Attn: R. P. Godwin)
118. Army Reactors Branch, AEC, Washington
119-120. New York Ship Building Corp., Camden, N. J. (Attn: E. L. Teale)
121-122. Research and Development Division, AEC, ORO
123-125. Reactor Division, AEC, ORO (Attn: D. F. Cope)
126-127. States Marine Corporation (Attn: R. D. Mehann)
128. The Babcock & Wilcox Company, Atomic Energy Division (Attn: D. W. Montgomery)
129-705. Given distribution as shown in TID-4500 (15th ed.) under Reactors–Power category (75 copies – OTS)